1 Introduction

The hygroscopicity of aerosol particles plays a critical role in visibility degradation, cloud formation, radiative forcing and thereby regional and global climate (Sloane and Wolff, 1985; Charlson et al., 1992; Pandis et al., 1995; Heintzenberg and Charlson, 2009; Shi et al., 2012). Also, the hygroscopic properties of aerosol determine which fraction of aerosol particles can act as cloud condensation nuclei (CCNs) and thus contribute to the aerosol indirect effect (Pilinis et al., 1995; McFiggans, 2006; Hallquist et al., 2009). Moreover, water uptake by aerosol particles influences their health effects, as reported in epidemiological studies (Pöschl, 2005). Therefore, understanding the interactions between water vapor and aerosol particles, as well as the related physicochemical processes in the atmosphere is of great significance.

Biomass burning is one of the important sources of anthropogenic atmospheric aerosols and also leads to the emission of greenhouse gases. The annual globally burned land area is in the range of 3 to 3.5 million square kilometers, resulting in emissions amounting to 2.5×10^9 kg carbon per year (van der Werf et al., 2006; Schultz et al., 2008). Particles in biomass burning smoke enriched with hygroscopic organic and inorganic constituents are suggested to act as efficient cloud condensation nuclei (Novakov and Corrigan, 1996; Petters et al., 2009; Rissler et al., 2010; Dusek et al., 2011; Frosch et al., 2011). In the Amazon basin, for example, the CCN concentration in the dry season is one order of magnitude higher than in the wet season due to biomass burning (Roberts et al., 2001; Carrico et al., 2008; Hening et al., 2010). In addition, the aerosol indirect climatic effects resulting from increased cloud condensation nuclei concentrations are expected to be very important in tropical regions, particularly in the regions with very high biomass

24 burning emissions (Roberts et al., 2001; Carrico et al., 2008; Hening et al., 2010).

25 Increased CCN concentrations may lead to reduced average cloud droplet radii and

26 associated with this, likely an enhanced negative radiative forcing of affected clouds

27 (Roberts et al., 2003; Lohmann and Feichter, 2005; Dinar et al., 2006a, b, 2007; Carrico

28 et al., 2008). Several groups have reported that a significant portion of particles in

29 biomass burning (from 11 % to as high as 99 % by mass) consists of water-soluble

30 organic carbon (WSOC) (Ruellan et al., 1999; Novakov and Corrigan, 1996; Narukawa et

31 al., 1999; Hoffer et al., 2006; Iinuma et al., 2007; Fu et al., 2009; Claeys et al., 2010;

32 Dusek et al., 2011; Psichoadaki and Pandis, 2013). For example, Andreae et al. (2002)

33 studied the chemical composition of the WSOC fraction of particles generated by

34 biomass burning and divided these detected WSOC into three different classes: (1)

35 neutrals (N), (2) monocarboxylic and dicarboxylic acids (MDA), and (3) polycarboxylic

36 acids (PA). Further, Artaxo et al. (2002) have suggested organic surrogate compounds

37 representing size-resolved WSOC chemical composition for the dry and wet seasonal

38 periods of their field campaign in Rondônia, Amazonia. On the basis of chemical

39 structure, these surrogate compounds can be represented approximately by: levoglucosan,

40 4-hydroxybenzoic acid, and humic acid (Hoffer et al., 2006). Sampled WSOC typically

41 contain the size distribution and a wide range of chemical species that are expected to

42 show rather different water solubilities, and different effect on the hygroscopic growth

43 factors of aerosol particles from biomass burning (Mochida and Kawamura, 2004; Biokos

44 et al., 2006; Rissler et al., 2010; Jung et al., 2011). However, for a variety of WSOC

45 compounds, it is not well known what the deliquescent relative humidity (DRH) of the

46 pure compound is, which determines if it can exhibit substantial water uptake at moderate

47 RH or not least as long as crystallization took place at dry conditions (followed by a

48 hydration trajectory). Some organic components that show a small solubility in pure

49 water (i.e., these require a large volume of water to be extracted and labeled as a WSOC),

50 may have a DRH close to 100 % RH, which is not accessible in our hydration

51 experiments (RH probed up to ~ 90 % RH). All these factors are of great importance in

52 determining the CCN activity of biomass burning particles.

53   Previous laboratory studies have addressed the effects of organic surrogate compounds

54 from biomass burning on the hygroscopic properties of mixed organic-inorganic aerosol

55 particles containing inorganic salts (Chan and Chan, 2003; Mochida and Kawamura,

56 2004; Brooks et al., 2004; Gysel et al., 2004; Chan et al., 2005; Svenningsson et al., 2005,

57 2006; Koehler et al., 2006; Badger et al., 2006; Dinar et al., 2007; Sjogren et al., 2007;

58 Carrico et al., 2008; Mikhailov et al. 2008, 2009; Hatch et al., 2009; Pope et al., 2010;

59 Zamora et al., 2011; Dusek et al., 2011; Frosch et al., 2011; Zamora and Jacobson, 2013).

60 Studies about the hygroscopicity of individual organic compounds characteristic to

61 biomass burning aerosol particles were performed by Mochida and Kawamura (2004).

62 Their results showed that the hygroscopic diameter growth factors of levoglucosan

63 aerosol particles are 1.23 at 80 % relative humidity (RH), while 4-hydroxybenzoic acid

64 does not show any hygroscopic growth up to 95% RH when starting with dry particles.

65 Water uptake by humic acid and mixtures of humic materials with ammonium sulfate

66 were determined using a HTDMA setup by Brooks et al. (2004). They showed that the

67 presence of humic acid affects the water uptake of mixed particles containing ammonium

68 sulfate + humic acid. However, actual biomass burning aerosols are typically much more

69 complex in terms of composition. The hygroscopicity of biomass burning aerosols likely

70 depends on the mixing of a diversity of organic compounds with inorganic constituents

71 during different time periods in the field (Decesari et al., 2006).

72   In this work, the hygroscopic properties of relevant organic compounds from biomass

73 burning are determined by the HTDMA technique. Using this experimental technique, we

74 also study the influence of the organic surrogate compounds on the water uptake behavior

75 of mixed organic-inorganic aerosols containing ammonium sulfate. Moreover, mixtures

76 of several the organic components with ammonium sulfate, mimicking more complex

77 particles observed in the atmosphere are investigated to determine the influence of

78 organic compounds on the overall particle hygroscopicity. In addition, we use the

79 Zdanovskii-Stokes-Robinson (ZSR) relation (Stokes and Robinson, 1966), the Extended

80 Aerosol Inorganic Model (E-AIM) (Clegg et al., 1992; Clegg et al., 2001; Clegg and

81 Seinfeld, 2006; available online: http://www.aim.env.uea.ac.uk/aim/aim.php), and the

82 Aerosol Inorganic-Organic Mixtures Functional groups Activity Coefficients

83 (AIOMFAC) model (Zuend et al., 2008, 2011) to predict the hygroscopic growth of

84 mixed aerosol particles and provide comparisons to our experimental findings.

85

86 **2 Experimental and modeling methods**

87

88 **2.1 HTDMA instrument setup and experimental protocol**

89

90 A schematic of our HTDMA setup is presented in Fig. 1. The HTDMA setup is

91 comprised of three main components: (1) the aerosol particle generation section, (2) the

92 particles sizing and humidification system and (3) a relative humidity control system.

93 Polydispersed sub-micrometer particles are generated using an atomizer (MSP 1500,

94   MSP) from bulk solutions (0.1 wt %) with different mass fractions of organic and

95   inorganic species with deionised water (EASY Pure® Ⅱ UF ultrapure water system, 18.2

96   MΩ cm), assuming that the compositions of the mixed aerosols remain the same as that

97   of the solution used in the atomizer. The aerosol particles pass through three silica gel

98   diffusion dryers (SDD) and a Nafion gas dryer (Perma Pure Inc., USA), bringing the

99   particles to a dry state ($RH_1 < 5$ %). The dry aerosols are subsequently charged and then

100   enter the first differential mobility analyzer (DMA1), where a near-monodisperse

101   distribution of particles of the desired dry diameter (D_0) of 100 ±1 nm is selected. After

102   size selection, aerosols are pre-humidified in a Nafion conditioner tube, and then flow

103   into a second Nafion tube at the set relative humidity, RH2, of a growth factor

104   measurement. the residence time of aerosol flow before entering into DMA2 is about 5 s

105   in the humidification section. This residence time may be insufficient for some organic

106   compounds to reach equilibrium at the high RH because of the very low accommodation

107   coefficient (Kerminen, 1997; Ha and Chan, 2001; Zhang and Chan, 2000; Peng and Chan,

108   2001; Chan et al., 2005). For example, for those coated with organic layers, $MgSO_4$,

109   sodium pyruvate, glutaric acid and asparagine. They need more long residence time to

110   reach equilibrium. Finally, the number size distributions for the humidified aerosols are

111   measured using the second DMA (DMA2) coupled with a condensation particle counter

112   CPC (Model 1500, MSP). The relative humidity of the DMA2 sheath flow, RH_3, is

113   measured using a dew point hygrometer (Michell, UK), with an uncertainty of ±0.08 %

114   RH. To allow the aerosol to equilibrate at the specified RH, we ensure that RH_3 is equal

115   to RH_2. In addition, critical orifices were used to regulate the sheath flows, which were

116   both recirculated using closed-loop arrangements (Jokinen and Makela, 1997).

117

2.2 Theory and modeling methods

The mobility-diameter growth factor is calculated as the ratio of mobility a particle established after exposure to a set RH level (mobility-diameter after humidification) to the reference mobility of the dry aerosol particles (at RH < 5 %). Hygroscopic diameter growth factors, $GF(\text{RH}) = D(\text{RH})/D_0$, where D(RH) is the particles diameter at a specific RH and D_0 the diameter at dry conditions (RH < 5 %), D_0 is often taken as the initial mode diameter of the aerosol ($D_{h,dry}$) at dry conditions, RH < 5 % selected by DMA1. In addition, following the definition of Mikhailov et al. (2004, 2008, 2009), a reference diameter D_0 can be defined as being the minimum diameter ($D_{h,min}$) observed while following an experimental protocol. The values of this minimum diameter and initial dry diameter are summarized in Table 2 (for set dry RH3 below 5 % RH in the HTDMA operation) and measured hygroscopic growth factor of compounds presented in Fig. 2. In addition, hydroscopic diameter growth factors are based on these reference minimum diameters for the pure components are predicted using different thermodynamic models and mixing rules. In each model, we assume that these particles are spherical. As a consequence, the predicated mobility equivalent diameter is equal to the volume equivalent diameter of a sphere.

2.2.1 *GF* data fit

An expression proposed by Dick et al. (2000) is used to present the relationship between water activity, a_w and $GF(\text{RH})$ for particles of individual compounds:

$$GF = \left[1 + \left(a + b * a_w + c * a_w^2 \right) \frac{a_w}{1 - a_w} \right]^{\frac{1}{3}} \tag{1}$$

139

$$RH / 100\% = a_w \times K_e \tag{2}$$

140

$$Ke = \exp\left\{ \frac{4\sigma_{sol} M_w}{RT\rho_w D_p} \right\} \tag{3}$$

141

142   Here a_w is the bulk water activity (mole fraction basis) at the composition of the solution

143   droplet corresponding to gas phase RH at equilibrium with a bulk solution, σ_{sol} is the

144   surface tension of the solution, M_w is the molecular weight of water, ρ_w is the density of

145   pure water at T, R is the universal gas constant, T is the temperature, D_p is the

146   sphere-equivalent mobility particle diameter, and K_e is the so-called Kelvin correction

147   factor term accounting for the droplet curvature.

148   The simplest assumption is that the Kelvin factor is equal to 1 (i.e., neglecting the droplet

149   curvature effect), applicable to the large particles, however, for 100 nm diameter particles,

150   ignoring the Kelvin effect at a given RH level and measured growth factor, leads to an

151   error in the corresponding bulk solution equivalent water activity of about 1 - 2 %

152   (Kreidenweis et al., 2005; Koehler et al., 2006). In this work, we have corrected all

153   HTDMA GF data by evaluating the Kelvin term (Eq. 3) for the retrieved droplet size at a

154   certain RH to obtain the corresponding water activity for comparison with models. The

155   coefficients a, b, and c of Eq. (1) are determined by fitting Eq. (1) to GF vs. a_w values

156   obtained by using Eq. (2) with measured GF data at known experimental RH level.

157   Equation (1) is appropriate to describe continuous water uptake behavior of particles

158   with a reference diameter at dry conditions (i.e., with $GF = 1.0$ at RH = 0 %).

159

160 **2.2.2 GF predictions by ZSR**

161 Assuming that the water uptake for each of the components of mixed particles can be

162 treated independently at a given RH, i.e., the assumption of the Zdanovskii, Stokes,

163 Robinson mixing rule, and that the partial volumes of individual components/phases are

164 additive, the GF of a mixture, GF_{mix}(RH), can be estimated from the GF_j of the pure

165 components j and their respective volume fractions, ε_j, in the mixture (Malm and

166 Kreidenweis, 1997):

167 $$GF_{mix} = \left[\sum_j \varepsilon_j \left(GF_j\right)^3\right]^{\frac{1}{3}} \qquad (4)$$

168

169 **2.2.3 GF prediction by E-AIM**

170 E-AIM is a thermodynamic equilibrium model used for calculating gas/liquid/solid

171 partitioning, widely used in the community. This model includes density predictions for

172 aerosol systems containing inorganic and organic components in aqueous solutions. This

173 allows for better consideration of non-ideal mixing effects on solution density, and hence

174 particle diameter at different RH. The group-contribution method UNIFAC (UNIversal

175 quasi-chemical Functional group Activity Coefficients) (Fredenslund et al., 1975; Hansen

176 et al., 1991), can be used within the E-AIM model to predict activity coefficients in

177 aqueous solutions of multifunctional organic compounds (Clegg et al., 2001). However,

178 the standard UNIFAC model (Fredenslund et al., 1975; Hansen et al., 1991) is usually not

179 appropriate for organic components in which two strongly polar groups are separated by

180 less than four carbon atoms giving rise to intramolecular interactions, such as hydrogen

181 bonding between certain polar groups. Some specific interaction parameters of UNIFAC

182 were revised by Peng et al (2001). The use of these modified UNIFAC parameters

183   improves the prediction of the water activity of dicarboxylic acids and

184   hydroxy-di-carboxylic and -tricarboxylic acids. These modified UNIFAC parameters can

185   also be chosen for calculations within the E-AIM model. The use of E-AIM model for

186   mixed organic-inorganic systems has been described in a range of papers (Hanford et al.,

187   2008; Clegg and Seinfeld, 2006; Hanford et al., 2008; Pope et al., 2010a; Yeung and

188   Chan, 2010).

189   We applied the E-AIM model to obtain the equilibrium state of aqueous mixtures and

190   predict the *GF* as a function of RH. The water uptake by the organic components is

191   estimated by choice with either the standard UNIFAC model or the modified UNIFAC

192   model with certain interaction parameters by Peng et al. (2001) UNIFAC-Peng as part of

193   the E-AIM model. Both flavours of UNIFAC have been applied for certain systems

194   studied in this work.

195

196   **2.2.4 *GF* prediction by AIOMFAC**

197   The AIOMFAC model by Zuend et al. (2008, 2011) is a thermodynamic

198   group-contribution model designed to calculate activity coefficient covering inorganic,

199   organic, and organic-inorganic interactions in aqueous solutions over a wide

200   concentration range. Like the optional choice in the E-AIM model, AIOMFAC also

201   includes a modified UNIFAC model. In addition, AIOMFAC includes long-range and

202   middle-range molecular interaction contributions based on a semi-empirical Pitzer-type

203   model expression to explicitly account for interactions between inorganic ions and

204   organic functional groups (plus water) in mixed solutions. This model has been

205   successfully applied to a variety of thermodynamic equilibrium calculations, including

206 the consideration of liquid-liquid phase separation and the deliquescence of ammonium

207 sulfate (e.g., Zuend et al., 2010; Song et al., 2012; Zuend and Seinfeld, 2012; Shiraiwa et

208 al., 2013).

209   In this study, we use a thermodynamic equilibrium model based on AIOMFAC (Zuend

210 and Seinfeld, 2012; Shiraiwa et al., 2013) which assumes that all components are in a

211 liquid or amorphous (viscous) solution, potentially exhibiting liquid-liquid phase

212 separation in a certain RH range – except for ammoniums sulfate, which, as an option, is

213 allowed to form a crystalline phase in equilibrium with the remaining solution (to

214 represent the efflorescence and deliquescence hysteresis behavior of the inorganic salt

215 depending on the mode of hydration/dehydration and starting RH in computations).

216 Liquid-liquid phase equilibria are predicted using the algorithm of Zuend and Seinfeld

217 (2013). However, the formation of solid (crystalline) organic phases is not generally

218 considered at this point since in actual complex organic aerosols, the formation of

219 crystalline organic phases is likely suppressed (Marcolli et al., 2004). Thus, in the context

220 of this study, where solid organic phases may be present in some of the systems, the

221 model will not be applicable – at least not to as part of the hydration branch of a humidity

222 cycle. As an exception, we apply the model for the mixed systems of 4-hydroxybenzoic

223 acid and ammoniums sulfate also in a mode where the assumption is made that the

224 organic component is solid and insoluble over the whole RH range considered (this

225 allows for better comparison with the experimental findings). Since this thermodynamic

226 model predicts the water content (mole fraction of water) of a mixture in equilibrium with

227 the gas phase at a given RH level, mass growth factors can be calculated directly.

228 However, to compute diameter growth factors, assumptions about the density of different

229   mixture components and non-ideal mixing effects on solution density need to be made.

230   Here we use the simplified assumption of additive component volumes, while accounting

231   for differences between the density of solid ammonium sulfate and dissolved aqueous

232   ammonium sulfate using pure component molar volume data reported by Lienhard et al.

233   (2012).

234

235   **2.2.5 Ideal solution growth factor**

236   The water activity of an ideal solution containing a nonvolatile, non-electrolyte

237   component is equal to the mole fraction of water (x_w) (activity coefficients of unity). Thus,

238   in the case of an ideal solution, we can estimate the water activity of liquid particles

239   directly from the knowledge of water content in term of x_w. Solutions comprising

240   electrolyte components, such as ammonium sulfate or sulfuric acid, are usually strongly

241   deviating from an ideal solution due to substantial dissolution (dissociation) of the

242   electrolytes and non-ideal interaction between ions, water, and organic compounds.

243   Therefore, water activities of mixed organic-inorganic systems may substantially differ

244   from a prediction by an ideal solution assumption (e.g., Zuend et al., 2011).

245   In this study, the ideal solution growth factor is used to explore its use as a simple

246   approach to describe the hygroscopic diameter growth factor of pure components and

247   mixtures, e.g. for ammonium sulfate and mixed particles. Since hygroscopic diameter

248   growth factor measurements using the HTDMA are on volume basis, the ideal solution

249   *GF* is calculated using mole fractions by the equation:

$$GF = \left[\frac{\sum_j \left(x_j M_j \dfrac{1}{\rho_j} \right)}{\sum_{j, j \neq w} \left(x_j M_j \dfrac{1}{\rho_j} \right)} \right]^{\frac{1}{3}}$$

250   (5)

251 Here, x_j, M_j, and $\rho_j$are mole fraction, molar mass and mass density of component j,

252 respectively. The sum in the numerator of Eq. (3) goes over all components including

253 water, while the sum in the denominator goes over all components except for water ($j \neq w$;

254 "dry" conditions). Note that when dissociated electrolyte components are present in the

255 liquid mixtures, the mole fractions in Eq. (3) have to be calculated as mole fractions with

256 respect to completely dissociated electrolytes (or an applicable degree of dissociation).

257 Equation (3) is more likely applicable when water and the solute components are in a

258 liquid solution, i.e., no solid /phases present. In addition, it is assumed that the partial

259 molar volumes of organics and water in solution are equal to those of the respective pure

260 liquid components.

261

262 **3 Results and discussion**

263 **3.1 *GF* of single solute systems**

264 The hygroscopic behavior of ammonium sulfate aerosol close to room temperature is well

265 understood and has been characterized by several groups (Gysel et al., 2002; Kreidenweis

266 et al., 2005; Biskos et al., 2006a, b). We can use it as a reference substance to calibrate

267 the HTDMA setup because of its well-known deliquescent point (80 % RH at 294.8 K)

268 (Onasch et al., 1999).

269   Fig. 2a. presents growth factors with respect to $D_0 = D_{h,dry}$ and $D_0 = D_{h,min}$ ammonium

270   sulfate particles from low to high RH . The measured growth factor of ammonium sulfate

271   is 1.45 ± 0.01 at 80% RH after deliquescence. The data agree well with values measured

272   by Gysel et al. (2002) and Wise et al. (2003), for example, the GF of AS is 1.45 at 24.9

273   ℃ as measured by Wise et al. (2003). In addition, the effects of particle shape/porosity

274   restructuring on hygroscopic behavior of AS particles investigated are rather small

275   (Mikhailov et al., 2004, 2008, 2009). The hygroscopic growth experiments for pure AS

276   are also in good agreement with the prediction from the E-AIM model and the

277   AIOMFAC model. Here, both models correctly account for the solid, crystalline state of

278   AS in the RH range before the deliquescence at ∼ 80 % RH for the conditions of a

279   hydration experiment. Slight differences between these two thermodynamic models,

280   which both account very well for the non-ideal solution behavior of AS, are due to

281   different conversions of mass growth to diameter growth factors by the models. The

282   E-AIM model includes a composition dependent solution density model, while the

283   AIOMFAC-based model simply assumes volume additivity (see discussion in Section

284   3.2). However, assuming an ideal solution, without consideration of the solid state and

285   mixing effects on solution density, its prediction for AS results in higher than measured

286   hygroscopic growth, also for RH > 80 %. Therefore, aside from the solid-to-liquid phase

287   transition, the water activity in concentrated solution also deviates from ideality.

288   As shown in Fig. 2b, levoglucosan aerosol particles show continuous water uptake

289   from low to high RH, and no deliquescence phase transition is observed, in excellent

290   agreement with the behavior reported by Mochida and Kawamura et al. (2004) and

291   Svenningsson et al. 2006. The measured *GF* at 80 % RH is 1.17 ±0.01, which is similar

292   to a result from the literature (Mochida and Kawamura, 2004), which report a growth

293   factor of levoglucosan of 1.18 at 80 % RH. Also, the measured hygroscopic growth

294   factors are reasonably consistent with those estimated from the standard UNIFAC model

295   within the E-AIM model, the AIOMFAC model, ideal solution theory, and the fitted

296   expression Eq. (1). At higher RH, deviations between the different models become more

297   significant for a good estimate of the actual GF. The measurements also suggest that

298   levoglucosan absorbs a small amount of water even at 5% RH, and that it remains liquid

299   over the full range of RH potentially rather viscous at lower RH. However, another

300   possible explanation for slight water uptake of levoglucosan could be that nanoparticles

301   produced by crystallization at very low RH contain volume and surface defects (porosity,

302   polycrystalline state), which may facilitate water adsorption followed by absorption

303   starting already at low relative humidity (Mikhailov et al., 2008, 2009). This possibility

304   cannot be ruled out by our measurements, but the observation, which do not show a

305   deliquescence step, would suggest that such an effect could only take place with a

306   gradual deliquescence in the levoglucosan system. Zuend et al. (2011) discuss the case of

307   AIOMFAC predictions for levoglucosan and its mixtures with different inorganic

308   electrolytes. They state that the molecular structure of levoglucosan with several polar

309   functional groups in close vicinity leads to less accurate model predictions for solutions

310   containing this compound. The same is true for UNIFAC model predictions and is

311   therefore a well-known limitation of these models for this particular system, explaining

312   the observed deviations between model curves and measurements.

313   As can be seen from Fig. 2c, humic acid aerosol particles show a slight increase in

314   GF from 10 % RH to 70 %. Above 70% RH, the particles start to take up increasingly

315   more water toward high RH. The effects of microscopic restructuring on the water uptake

316   of humic acid aerosol particles are relatively the same small, comparable with those of

317   ammonium sulfate and levoglucosan aerosol particles. A similar tendency had been

318   observed by Brooks et al. (2004), However, a contrasting phenomenon was observed by

319   Zamora and Jacobson (2013); no hygroscopic growth of humic acid particles was

320   observed over the full range of RH in their study. Due to the lack of detailed physical and

321   chemical information about the used humic acid, the *GF* of humic acid particles are only

322   presented with a data fit based on Eq. (1). The determined fit parameters are listed in

323   Table 2. For model calculations with E-AIM and AIOMFAC, the chemical structure or at

324   least the type and relative abundance of functional groups needs to be known, which is

325   not the case for the humic acid particles.

326   The hygroscopic growth curves for 4-hydroxybenzoic acid are presented in Fig. 2d. No

327   hygroscopic growth (within error) was observed below 90 % RH. Measured hygroscopic

328   diameter growth factors with respect to $D_{h,min}$ are above 1.0, and are close to 1.0 toward

329   high RH (the minimum diameter was found at the highest RH measured). The main

330   reasons for the observation of smaller particles at higher RH is likely the restructuring

331   and/or partial evaporation of particles at higher relative humidity in the hydration mode.

332   The measured hygroscopic diameter growth factor with respect to $D_{h,dry}$ show of course

333   the same slight decrease in particles diameter with increasing RH. with this definition of

334   the reference diameter leading to GF smaller than 1.0 at higher RH, which is consistent

335   with previous experiments by another group (Mochida and Kawamura, 2004). The

336   reasons for the decrease in particle diameter are not fully understood, but the same

337   behavior is reported by Shi et al. (2012) for particles consisting of ammonium sulfate +

benzoic acid. On the basis of Transmission electron microscopy (TEM) image analysis, they attribute the diameter decrease to the microscopic restructuring of solid particles with increasing RH, which may affect the particle mobility diameter. Therefore, a similar effect could be responsible for the observations from our experiments. Another potential reason for a decrease in apparent diameter could be the partial evaporation of semivolatile organics from the aerosol particles in the HTDMA (here: 4-hydroxybenzoic acid, pure liquid vapour pressure $p^{0,L} = 8.11 \times 10^{-4}$ Pa at 298.15 K, Booth et al. (2012)), an effect that is also known for certain volatile inorganic particles (e.g., NH_4NO_3) (Lightstone et al., 2000; Hersey et al., 2013). In order to probe hysteresis effects of 4-hydroxybenzoic acid during hydration and dehydration processing of the aerosol, another experiment was conducted for 4-hydroxybenzoic acid. First, the 4-hydroxybenzoic acid aerosol particles were passed through a water supersaturation humidifier (RH of above 100 %), followed by drying to the different RH setpoints (90 % to 5 % RH). No obvious diameter changes other than potential restructuring effects were observed in this experiment. A possible reason is that the particles deliquesce in the oversaturation humidifier, but that their efflorescence occurs above 90 % RH, likely even above 97 % RH by their efflorescence (Mochida and Kawamura, 2004). A second possible issue could be that the residence time in the humidifier section (~ 5 s) of our HTDMA setup is too short for 100 nm 4-hydroxybenzoic acid particle to fully deliquesce. Our observations of this very limited solubility of 4-hydroxybenzoic acid, and hence, a high DRH are in agreement with the experimental data of Mochida and Kawamura (2004) for this system. Obviously, the observed results are different from the GF curves predicted by the ideal solution theory, the AIOMFAC model, and the UNIFAC-Peng

361 (within E-AIM) model. For these predictions hydration mode, starting with particles at 0

362 % RH, the applied models assume that the organic component is present in the liquid

363 state and that solid organic phases are not present. However, the experimental data

364 indicate that 4-hydroxybenzoic acid is solid and remains solid in the range from 5 % to

365 90 % RH for a hydration experiment. Hence, the shown model predictions clearly deviate

366 from the measurements due to the unfavourable assumption of a liquid solution and not

367 because of a general limitation of the models for describing growth factors of the aqueous

368 4-hydroxybenzoic acid. Would the models account for a solid organic phases, the

369 predicted GF would be 1.0 throughout the showed experimental RH range with

370 deliquescence of the organic crystal expected to occur at an RH value greater than 90 %.

371 Indeed, the model curves may well capture the water uptake/loss behavior prior to

372 crystallization for the case of a dehydration experiment starting at very high RH ($\sim$ 100

373 %) with liquid particles becoming supersaturated, metastable solution as RH is decreased

374 below the deliquescence point).

375 **3.2 Mixed systems: ammonium sulfate + levoglucosan**

376 The measured water uptake by 100 nm particles consisting of different mixtures of

377 ammonium sulfate + levoglucosan with dry mass ratios of 3:1, 1:1, and 1:3, shown in Fig.

378 3, present a reduction in the *GF* at RH > 80 % with increasing levoglucosan mass fraction

379 and therefore decreasing AS content. For example, the growth factors are 1.30, 1.30, and

380 1.28 at 80 % RH, respectively, relative to the *GF* of 1.45 of pure AS particles at 80 % RH.

381 there is a clear shift in the full deliquescence of AS at RH= ~ 80 % RH to lower RH with

382 increasing levoglucosan mass fraction, which indicates the levoglucosan aerosol particles

383 have significant effect on the deliquescence of ammonium sulfate. And with increasing

17

384 levoglucosan mass fraction, the smoothing of hygroscopic behavior is obvious. this

385 phenomenon was observed for mixtures of ammonium sulfate and succinic acid, malonic

386 acid, monomethylaminium sulfate (MMAS), dimethylaminium sulfate (DMAS) by

387 previous studies (e.g., Zaedini et al., 2008; Hämer et al., 2002; Qiu and Zhang, 2013). For

388 example, Qiu and Zhang (2013) observed that particles consisting of 10 wt % MMAS, or

389 DMAS and ammonium sulfate exhibit a moderate growth by water uptake in the RH

390 range of 40 - 70 % RH. In addition, the hygroscopicity of internal mixtures of ammonium

391 sulfate aerosol and levoglucosan with core-shell and well-mixed mixing structures were

392 performed by Maskey et al. (2014) using HTDMA technique. They showed that the GF

393 of the well-mixed particles was higher than that of the core-shell particles with the same

394 fraction volume.

395 The experimental hygroscopic growth results for AS + levoglucosan mixtures are

396 compared with four models predictions. The E-AIM model with standard UNIFAC is in

397 relatively good agreement with the measured hygroscopic growth factors, but slightly

398 overestimating the water uptake at RH < ~ 70 %. Especially in the case of the 1 : 1

399 mixtures of AS: levoglucosan (by mass), the E-AIM model includes a composition

400 dependent solution density model, (i.e., solution density depends on water content and

401 therefore RH), while the AIOMFAC-based model does not include such a sophisticated

402 treatment. The AIOMFAC model assumes linear additivity of pure component liquid or

403 solid volumes/density to estimate the droplet diameter at a given RH. A possible reason

404 for small differences between the model predictions is that E-AIM model provides

405 droplet volume output based on density predictions of the aqueous system at different

406 compositions (Clegg and Wexler, 2011a, b), while the other two models use a simpler

volume additivity approach. We attribute a small effect on predicted GF curves due to different density treatment in E-AIM and the AIOMFAC-based model based on a comparison of E-AIM and AIOMFAC-based predicted mass growth factors and diameter growth factors for pure ammonium sulfate shown in Fig. 7.. In the case of predicted mass growth factors of ammonium sulfate, both models agree very well with each other, indicating the slight differences in predicted diameter growth factors must be due to the different way the conversion from particle mass to particle volume is done in the two models. In addition, for the levoglucosan + AS mixtures, the AIOMFAC-based model predicts a liquid-liquid phase separation between 80 % and ~ 90 % RH for the hydration conditions. The E-AIM model does not predict a phase separation and estimates a higher miscibility between the inorganic and organic components, which seems to be in better agreement with the experimental data. This is the major reason for the differences between the two model predictions regarding the diameter growth factors above AS deliquescence in case of the levoglucosan + AS system. In addition, the E-AIM model predicts a slightly higher mutual solubility of AS and levoglucosan at RH < 80 % in comparison to AIOMFAC, which leads to more dissolution of AS and associated with that, to a large water uptake at RH below full deliquescence. Regarding the ideal solution curve without consideration of a solid AS phase, the ideal curve approaches better with the measured GFs with increasing mass fraction of levoglucosan, which is a consequence of a reduced effect and less abrupt deliquescence transition of ammonium sulfate in the mixtures with higher levoglucosan mass fraction. The ZSR model is based on hygroscopic growth factors of ammonium sulfate and levoglucosan derived from E-AIM predictions for AS and fitted *GF* curve (Eq. 1) for levoglucosan. At RH above 80 %, the

430   ZSR model is in relatively good agreement with the measured particle hygroscopicities

431   when accounting for measurement error. However, due to the nature of the classical ZSR

432   model used, the mutual solubility of AS in aqueous levoglucosan solution at RH < 80 %

433   below full AS deliquescence is not considered, i.e., the water uptake of organic and

434   inorganic components is treated separately and no dissolution effects are accounted for.

435   At those lower RH conditions, this leads to the largest deviations from experimental data

436   for the ZSR predictions in comparison to the two other models.

437   **3.3 Mixed systems: ammonium sulfate + humic acid**

438   Hygroscopic behavior of 100 nm particles containing ammonium sulfate + humic acid

439   with dry mass ratios of 3:1, 1:1, 1:3, shown in Fig.4, present a reduction in GF at RH >

440   80 % with increasing mass fraction of HA (decreasing AS content). For instance, the

441   measured growth factors are 1.30, 1.21, and 1.18 at 80 % RH after full AS deliquescence

442   for the particles containing 25 wt%, 50 wt% and 75 wt% HA (dry composition)

443   compared to a growth factor of 1.45 for pure, deliquesced AS particles at 80 % RH.

444   Adding HA causes the mixed particles to start to take up a small amount of water before

445   the complete deliquescence of AS, indicating HA aerosol particles have a litter effect on

446   the deliquescence of AS. A similar tendency had been observed by Brooks et al. (2004)

447   for mixtures containing HA and AS, which exhibit a size growth prior to 80 % RH.

448   Hygroscopic growth factors referring to the water uptake contribution by HA in the ZSR

449   relation are obtained from the fitted growth curve of pure HA particles (Eq. 1). As for the

450   humic acid + AS system, E-AIM predictions of the growth factors of pure AS are used in

451   the ZSR relation here. The resulting ZSR prediction agrees relatively well with the

452   measured hygroscopic growth of the different mixtures. Also qualitatively, when

453   comparing the three mixtures, the ZSR prediction reproduces the lower *GF* of the 3:1

454   AS:HA particles at RH < 80 % least amount of HA and then by contrast the higher *GF*

455   for RH > 80 % due to a large water uptake contribution from AS after deliquescence.

456   Model predictions using the E-AIM and AIOMFAC could not be performed for this

457   system because of the lack of knowledge about the actual molecular structure of the

458   humic acid samples used.

459   **3.4 Mixed systems: ammonium sulfate + 4-hydroxybenzoic acid**

460   Figure 5 shows the measurement and model predictions for particles consisting of

461   ammonium sulfate + 4-hydroxybenzoic acid with dry mass ratios of 3:1, 1:1, 1:3, A *GF*

462   reduction from panels (a) to (c) at high relative humidity is mainly due to an increasing

463   mass fraction of 4-hydroxybenzoic acid. For example, the measured growth factors are

464   1.31, 1.26, and 1.10 at 80 % RH after full AS deliquescence for the particles containing

465   25 wt%, 50 wt%, and 75 wt% 4-hydroxybenzoic acid (dry mass percentages),

466   respectively. Hygroscopic behavior of mixed 4-hydroxybenzoic acid – AS particles is

467   found to be essentially unaffected by the presence of 4-hydroxybenzoic acid.

468   4-hydroxybenzoic acid aerosol particles have no influence on the deliquescence point of

469   ammonium sulfate with the low water solubility. Similar phenomenon was observed for

470   mixtures of ammonium sulfate and organics containing glutaric, pinonic acid, and

471   phthalic acid with low water solubility by Cruz and Pandis 2000 and Hamer et al. 2002

472   However, the GF of such particles differ from pure AS particles due to the different basis

473   of normalization dry diameter includes insoluble organic phase for the same dry size

474   particles class. The ZSR relation agrees very well with the measured hygroscopic growth

475   for mixed particles within measurement error due to fitted hygroscopic growth factors for

476 4-hydroxybenzoic acid are used as input for the ZSR relation (Eq. 2). For the case of

477 particles containing AS and 4-hydroxybenzoic acid, the ideal solution curves shows a

478 large deviation from measured *GFs*, partly because of the solid organic phase, but it is

479 also obvious that such mixtures deviate from ideal behavior. As in the case of binary

480 4-hydroxybenzoic acid + water system (Fig. 2d), for the mixed systems with ammonium

481 sulfate (Fig. 5), E-AIM model predictions are referring to a system where the organic

482 component remains liquid at all RH, i.e., without consideration of a solid organic phase

483 that is most likely present during these hydration experiments. However, the

484 crystallization and dissolution of ammonium sulfate is considered by the two

485 thermodynamic models. Hence, the systematic offset observed when comparing model

486 results and measurements in Fig. 5 is mainly due to incorrect model assumptions for

487 these organic-inorganic mixtures. In the case of the AIOMFAC model prediction a solid

488 organic phase is assumed, i.e., it is assumed that the organic growth factor contribution

489 *GF* (4-hydroxybenzoic acid) =1.0 for the whole RH range, the resulting particle growth

490 prediction is still a bit higher than the measured hygroscopic particle growths above 80 %

491 RH.This is largely explained by the fact that the measurement indicate *GF* < 1.0 at RH

492 $\approx$ 80 % and above, potentially due to particles morphology effects, which then presents

493 a systematic offset between measurements and model prediction. Microscopical particle

494 morphology restructuring and associated size changes of solid particles at moderate to

495 high RH levels have been found in other experiments too. An interesting, yet contrasting

496 phenomenon was observed by Sjogren et al. (2007). They investigated different mixtures

497 of ammonium sulfate + adipic acid in the RH range from $\sim$ 5 % to $\sim$ 95 % using

498 HTDMA instruments and an electrodynamic balance (EDB). In addition, Sjogren et al.

499 (2007) studied the morphology of samples of their mixed aerosols containing solid

500 (insoluble) adipic acid using scanning electron microscopy (SEM). Growth factors

501 indicating significant water uptake at RH below the full deliquescence of AS and

502 systematic deviations from ZSR predictions observed are explained by Sjogren et al.

503 (2007) as a result of morphological effects, including an inverse Kelvin effect, leading to

504 enhanced particle growth factors due to water uptake into cracks, veins and pores of

505 polycrystalline solids. In contrast, our observations indicate a shrinking of

506 4-hydroxybenzoic acid containing particles with increasing RH or at least a decrease of

507 their mobility-equivalent diameters.

3.5 Mixtures of biomass burning organic surrogate compounds with ammonium

sulfate

510 The water soluble organic carbon (WSOC) fraction in biomass burning aerosol is mainly

511 composed of neutral compounds, a large fraction of which consisting of sugar-like

512 compounds such as levoglucosan, mannosan and D-glucose. Levoglucosan, a major

513 pyrolysis product of cellulose and hemicellulose, contributes substantially (16 %-31 % by

514 mass) to the total organic fraction in $PM_{2.5}$ (Mochida and Kawamura, 2004; Iinuma et al.,

515 2007; Claeys et al., 2010; Engling et al., 2013; Samburova et al., 2013). In general, MDA

516 have been identified as pyrolysis products of lignin, which is a major constituent of

517 woods (Mochida and Kawamura, 2004; Hoffer et al., 2006; Iinuma et al., 2007; Fu et al.,

518 2009; Dusek et al., 2011; Psichoadaki and Pandis. 2013). We use 4-hydroxybenzoic acid

519 to represent as a surrogate the MDA fraction; The polyacidic (PA) fraction of organic

520 compounds is found in all samples of biomass burning aerosols (Decesari et al., 2006).

521 Using the H-NMR technique for aerosol analysis of samples from the Po valley in Italy

522 more than 40% of the water soluble organic carbon was identified as PA having

523 molecular structures similar to humic materials (HMs) (Decesari et al., 2002; Fuzzi1 et

524 al.,2001; Dinar et al., 2006a, b, 2007; Pope et al., 2010; Zamora et al., 2011; Fors et al.,

525 2010). Therefore, organic surrogate compounds (levoglucosan, 4-hydroxybenzoic acid,

526 and humic acid) have been proposed to represent the composition of WSOC on the basis

527 of speciation methods and functional groups analysis (Decesari et al., 2006). The effects

528 of such organic surrogate compounds on the hygroscopic behavior of mixed

529 organic-inorganic particles containing also ammonium sulfate are measured and

530 discussed in following. We use the relative abundances of the three model compound

531 classes based on the chemical composition analysis of atmospheric particles reported by

532 the Decesari et al. (2006). The chemical compositions of two distinct mixtures are given

533 in Table 2. Mix-bio-dry and mix-bio-wet are compositions typical of biomass burning

534 aerosols in the two different seasons (dry and wet) in the Amazon basin near Rondônia,

535 Brazil (Decesari et al., 2006).

536 **3.5.1 Water uptake of mix-bio-dry and mix-bio-wet particles**

537 The hygroscopic behavior of mix-bio-dry particles in terms of *GF* is presented in Fig. 6a.

538 Mixtures of organic surrogate compounds and AS in these dry season model particles do

539 not show any growth below 65 % RH. However, mix-bio-dry particles begin to take up

540 water at 65% RH and show steep growth between 75 % and 80 % RH, where the partial

541 deliquescence of AS contributes increasingly to the water uptake and, hence, the overall

542 growth factor. Similar water uptake behavior prior to full AS deliquescence has been

543 reported by Zardini et al. (2008) and Wu et al. (2011) for different organic + ammonium

544 sulfate mixed aerosol systems. The E-AIM model prediction for mixtures consisting of

545   ammonium sulfate + levoglucosan with a comparable dry mass percentage ratio of 68

546   wt%: 26 wt% is in relatively good agreement with the measured growth factors above 75

547   % RH, this reveals that levoglucosan, as part of the mixture of organic biomass burning

548   organic surrogate compounds, largely contributes to the water uptake of mixtures

549   containing organic surrogate compounds and ammonium sulfate before the deliquescence

550   of AS. The ZSR model curve is calculated on the basis of the growth factors of the pure

551   components: for AS using E-AIM, for levoglucosan, 4-hydroxybenzoic acid and humic

552   acid using the fitted expression (Eq. 1). The ZSR prediction tends to agree well with the

553   water uptake investigated at RH above 80 % RH, while large deviations are found for the

554   range between 0 % and 80 % RH, for similar reasons as discussed for the AS +

555   levoglucosan systems (Fig. 3 and related text).

556   The hygroscopic behavior of mix-bio-wet particles is shown in Fig. 6b. In contrast to

557   mix-bio-dry particles, mix-bio-wet aerosols show little water uptake below 80 % RH.

558   This result is expected given the lower mass fraction of hygroscopic organics (e.g., only

559   9.2 wt % levoglucosan) in the mix-bio-wet particles. The observed hygroscopic behavior

560   of mixed organic-inorganic aerosols of other HTDMA studies on biomass burning

561   aerosols published in the literature, e.g, Wu et al. (2011), cannot be compared directly to

562   our measurements, because the samples and organic : inorganic rations are different.

563   However, the work by Wu et al. (2011) shows that other mixtures containing AS and

564   organic acids found in biomass burning aerosol from Brazil, show significant water

565   uptake at relative humidities below 80 %, similar to our mix-bio-dry case. In addition, the

566   E-AIM model prediction for mixtures consisting of AS and levoglucosan by mass

567   percentage ratio of 87 wt% : 9.2 wt% is in good agreement with the measured growth

568   curve, which indicates that levoglucosan mainly contributes to the hygroscopic behavior

569   of the organic aerosol fraction of the mixtures consisting of biomass burning model

570   organics and AS. Also, due to the limited water uptake prior to AS deliquescence in the

571   mix-bio-wet case, the ZSR prediction results in a good description of the measured

572   growth curve.

573   To summarize, the hygroscopic growth factor of mixed organic + ammonium sulfate

574   particles is affected by the presence and relative composition of organic surrogate

575   compounds from biomass burning. For example, the growth factors during humidification

576   of mixed particles composed of model organics and AS at 80 % RH are 1.35 for

577   representative dry season aerosols and 1.37 for wet season aerosols. These growth factors

578   are lower than the *GF* of 1.45 for pure AS particles, which is of course expected given

579   the lower hygroscopicity of the organic components and the general finding that water

580   uptake contributions according to Eq. (2) usually describes a mixture's *GF* quite well.

581   The measured *GF* values of our biomass burning model systems are similar to the ones

582   reported by Jung et al. (2011) for biomass burning aerosols sampled in Ulaanbaatar,

583   Mongolia, for which the *GF* were found to be between 1.30 and 1.35 at 80 % RH during

584   hydration. Effects of organic surrogate compounds on the deliquescence behavior of AS

585   are found with increasing mass fraction of hygroscopic organic surrogate compounds,

586   particularly levoglucosan, from aerosol mixtures representing the wet and dry seasons in

587   the Amazon basin. In the case of dry period aerosols with an enhanced mass fraction of

588   organic surrogate compounds, a smoothing of the hygroscopic behavior is observed,

589   likely due to the continuous water uptake by levoglucosan and partial dissolution and

590   additional water uptake by ammonium sulfate. This result is similar to the observed

591   behavior in simple, binary mixtures of levoglucosan + AS, suggesting that

592   4-hydroxybenzoic acid and HA show little to no effect on the hygroscopic behavior of

593   mixed particles during a hydration experiment starting at dry conditions.

594   **4 Conclusions**

595   According to field studies reported in the literature, aerosol particles from biomass

596   burning events always contain a variety of inorganic and organic compounds. Different

597   compositions of these aerosol particles have a significant influence on their

598   physicochemical properties, in particular hygroscopic behavior. Differences regarding

599   aerosol number concentration and particle composition were observed for the dry and wet

600   seasons in the Amazon and other regions (Artaxo et al., 2002; Decesari et al., 2006;

601   Rissler et al., 2006). In this work, we focused on three organic compounds (levoglucosan,

602   4-hydroxybenzoic acid, and humic acid) to represent common compound classes from

603   biomass burning. These organics are also representative of three different water uptake

604   characteristics. Hygroscopic growth measurement for the two-component organic + AS

605   particles show that certain organic compounds can have an important influence on the

606   overall particle diameter growth factor and the partial deliquescence of AS, e.g., mixtures

607   of levoglucosan with AS. With increasing mass fraction of levoglucosan, a clear shift of

608   the onset of AS deliquescence to lower RH is occurring, which also leads to an overall

609   more smooth looking hygroscopic growth factor curve. In contrast, 4-hydroxybenzoic

610   acid and humic acid show no obvious effect on the deliquescence RH of AS. Also, due to

611   the limited solubility of these two organic compounds, the hygroscopic growth factors at

612   RH below 95 %, as measured, are reduced relative to that of pure AS particles.

613   Mixtures of organic surrogate compounds with AS, representing atmospheric aerosols

614   from biomass burning were made, with chemical compositions determined on the basis of

615   different organic and inorganic component fractions observed for the dry and the wet

616   period in the Amazon basin. The most striking difference in measured hygroscopic

617   growth curves comparing the two seasons is due to presence of different amounts of

618   levoglucosan as surrogate compound, implying that highly oxidized organic compounds

619   like levoglucosan may play an important role in controlling the hygroscopic behavior of

620   atmospheric particles at RH below the full deliquescence of inorganic salts, such as AS.

621   Therefore, a main advantage of using organic surrogate compounds representing the

622   complex WSOC fraction of biomass burning, aerosol is their use for laboratory

623   experiments and associated evaluation and improvement of thermodynamic mixing

624   models and parameterization for the predictions of hygroscopic behavior and CCN

625   activity in atmospheric models.

626   This work focuses on the water uptake and deliquescence behavior of organic

627   compounds from biomass burning sources and their influence on the water uptake of

628   mixed organic-ammonium sulfate aerosol particles. Ambient biomass burning aerosol

629   particles may undergo the humidity cycles depending on the RH history of an air parcel.

630   Humidity cycles may possible lead to solid-liquid phase transition hysteresis with distinct

631   deliquescence and efflorescence behavior of the organic components and

632   organic-inorganic-mixtures. Associated changes of aerosol hygroscopicity of mixed

633   particles similar to the multicomponent systems studies in this work will be a topic of

634   studies in the future.

635

References

Abbatt, J. P. D., Broekhuizen, K., and Kumal, P. P.: Cloud condensation nucleus activity of internally mixed ammonium sulfate/organic acid aerosol particles, Atmospheric Environment, 39, 4767-4778, 10.1016/j.atmosenv.2005.04.029, 2005.

Agarwal, S., Aggarwal, S. G., Okuzawa, K., and Kawamura, K.: Size distributions of dicarboxylic acids, ketoacids, α-dicarbonyls, sugars, WSOC, OC, EC and inorganic ions in atmospheric particles over Northern Japan: implication for long-range transport of Siberian biomass burning and East Asian polluted aerosols, Atmospheric Chemistry and Physics, 10, 5839-5858, 10.5194/acp-10-5839-2010, 2010.

Andreae, M. O., Artaxo, P., Brandao, C., Carswell, F. E., Ciccioli, P., da Costa, A. L., Culf, A. D., Esteves, J. L., Gash, J. H. C., Grace, J., Kabat, P., Lelieveld, J., Malhi, Y., Manzi, A. O., Meixner, F. X., Nobre, A. D., Nobre, C., Ruivo, M., Silva-Dias, M. A., Stefani, P., Valentini, R., von Jouanne, J., and Waterloo, M. J.: Biogeochemical cycling of carbon, water, energy, trace gases, and aerosols in Amazonia: The LBAEUSTACH experiments, J. Geophys. Res.-Atmos., 107, 8066, doi:10.1029/2001JD000524, 2002.

Artaxo, P., Martins, J. V., Yamasoe, M. A., Procopio, A. S., Pauliquevis, T. M., Andreae, M. O., Guyon, P., Gatti, L. V., and Leal, A. M. C.: Physical and chemical properties of aerosols in the wet and dry seasons in Rondonia, Amazonia, J. Geophys. Res.-Atmos., 107, 8081. doi:10.1029/2001jd000666, 2002.

Badger, C. L., George, I., Griffiths, P. T., Braban, C. F., Cox, R. A., and Abbatt, J. P. D.: Phase transitions and hygroscopic growth of aerosol particles containing humic acid and mixtures of humic acid and ammonium sulphate, Atmospheric Chemistry and

659   Physics, 6, 755-768, 2006.

660   Beyer, K. D., Friesen, K., Bothe, J. R., and Palet, B.: Phase Diagrams and Water

661   Activities of Aqueous Dicarboxylic Acid Systems of Atmospheric Importance, Journal

662   of Physical Chemistry A, 112, 11704-11713, 10.1021/jp805985t, 2008.

663   Biskos, G., Paulsen, D., Russell, L. M., Buseck, P. R., and Martin, S. T.: Prompt

664   deliquescence and efflorescence of aerosol nanoparticles, Atmospheric Chemistry and

665   Physics, 6, 4633-4642, 2006a.

666   Biskos, G., Russell, L. M., Buseck, P. R., and Martin, S. T.: Nano-size effect on the

667   hygroscopic growth factor of aerosol particles, Geophys. Res. Lett., 33, L07801,

668   doi:10.1029/2005GL025199, 2006b.

669   Brooks, S. D., DeMott, P. J., and Kreidenweis, S. M.: Water uptake by particles

670   containing humic materials and mixtures of humic materials with ammonium sulfate,

671   Atmospheric Environment, 38, 1859-1868, 10.1016/j.atmosenv.2004.01.009, 2004.

672   Carrico, C. M., Petters, M. D., Kreidenweis, S. M., Collett, J. L., Engling, G., and Malm,

673   W. C.: Aerosol hygroscopicity and cloud droplet activation of extracts of filters from

674   biomass   burning   experiments,   Journal   of   Geophysical   Research,   113,

675   10.1029/2007jd009274, 2008.

676   Chan, M. N., and Chan, C. K.: Hygroscopic properties of two model humic-like

677   substances   and   their   mixtures   with   inorganics   of   atmospheric   importance,

678   Environmental Science & Technology, 37, 5109-5115, 10.1021/es034272o, 2003.

679   Chan, M. N., Choi, M. Y., Ng, N. L., and Chan, C. K.: Hygroscopicity of water-soluble

680   organic compounds in atmospheric aerosols: Amino acids and biomass burning derived

681   organic   species,   Environmental   Science   &   Technology,   39,   1555-1562,

682   10.1021/es049584l, 2005.

683   Chan, M. N., Lee, A. K. Y., and Chan, C. K.: Responses of ammonium sulfate particles

684   coated with glutaric acid to cyclic changes in relative humidity: Hygroscopicity and

685   Raman characterization, Environmental Science & Technology, 40, 6983-6989,

686   10.1021/es060928c, 2006.

687   Chan, M. N., and Chan, C. K.: Mass transfer effects in hygroscopic measurements of

688   aerosol particles, Atmospheric Chemistry and Physics, 5, 2703-2712,2005.

689   Charlson, R. J., Schwartz, S. E., Hales, J. M., Cess, R. D., Coakley, J. A., Hansen, J. E.,

690   and Hofmann, D. J.: Climate forcing by anthropogenic aerosols, Science, 255, 423-430,

691   10.1126/science.255.5043.423, 1992.

692   Claeys, M., Kourtchev, I., Pashynska, V., Vas, G., Vermeylen, R., Wang, W., Cafmeyer, J.,

693   Chi, X., Artaxo, P., Andreae, M. O., and Maenhaut, W.: Polar organic marker

694   compounds in atmospheric aerosols during the IBA-SMOCC 2002 biomass burning

695   experiment in Rondônia, Brazil: sources and source processes, time series, diel

696   variations and size distributions, Atmospheric Chemistry and Physics, 10, 9319-9331,

697   10.5194/acp-10-9319-2010, 2010.

698   Clegg, S. L., Pitzer, K. S., and Brimblecombe, P.: thermodynamics of multicomponent,

699   miscible, ionic-solutions electrolytes. 2. mixtures including unsymmetrical electrolytes,

700   Journal of Physical Chemistry, 96, 9470-9479, 10.1021/j100202a074, 1992.

701   Clegg, S. L., Seinfeld, J. H., and Brimblecombe, P.: Thermodynamic modelling of

702   aqueous aerosols containing electrolytes and dissolved organic compounds, Journal of

703   Aerosol Science, 32, 713-738, 10.1016/s0021-8502(00)00105-1, 2001.

704   Clegg, S. L., Seinfeld, J. H., and Edney, E. O.: Thermodynamic modelling of aqueous

705   aerosols containing electrolytes and dissolved organic compounds. II. An extended

706   Zdanovskii-Stokes-Robinson approach, Journal of Aerosol Science, 34, 667-690,

707   10.1016/s0021-8502(03)00019-3, 2003.

708 Clegg, S. L., and Seinfeld, J. H.: Thermodynamic models of aqueous solutions containing

709   inorganic electrolytes and dicarboxylic acids at 298.15 K. 2. Systems including

710   dissociation equilibria, Journal of Physical Chemistry A, 110, 5718-5734,

711   10.1021/jp056150j, 2006a.

712 Clegg, S. L. and Seinfeld, J. H.: Thermodynamic models of aqueous solutions containing

713   in-organic electrolytes and dicarboxylic acids at 298.15 K. 2. Systems including

714   dissociation equilibria, J. Phys. Chem. A, 110, 5718–5734, doi:10.1021/jp056150j,

715   2006b.

716 Clegg, S. L., and Wexler, A. S.: Densities and apparent molar volumes of atmospherically

717   important electrolyte solutions. 2. The systems H^+-HSO_4^--SO_4^{2-}-H_2O from 0 to 3 mol

718   kg^{-1} as a function of temperature and H^+-NH_4^+-HSO_4^--SO_4^{2-}-H_2O from 0 to 6 mol kg^{-1}

719   at 25 degrees C using a Pitzer ion interaction model, and NH_4HSO_4-H_2O and

720    $(NH_4)_3H(SO_4)_2$-H_2O over the entire concentration range, The journal of physical

721   chemistry. A, 115, 3461-3474, 10.1021/jp1089933, 2011a.

722 Clegg, S. L., and Wexler, A. S.: Densities and Apparent Molar Volumes of

723   Atmospherically Important Electrolyte Solutions. 1. The Solutes H_2SO_4, HNO_3, HCl,

724   Na_2SO_4, $NaNO_3$, NaCl, $(NH_4)_2SO_4$, NH_4NO_3, and NH_4Cl from 0 to 50 degrees C,

725   Including Extrapolations to Very Low Temperature and to the Pure Liquid State, and

726    $NaHSO_4$, NaOH, and NH_3 at 25 degrees C, Journal of Physical Chemistry A, 115,

727   3393-3460, 10.1021/jp108992a, 2011b.

728   Cruz, C. N., and Pandis, S. N.: The effect of organic coatings on the cloud condensation

729   nuclei activation of inorganic atmospheric aerosol, Journal of Geophysical

730   Research-Atmospheres, 103, 13111-13123, 10.1029/98jd00979, 1998.

731   Decesari, S., Facchini, M. C., Matta, E., Mircea, M., Fuzzi, S., Chughtai, A. R., and

732   Smith, D. M.: Water soluble organic compounds formed by oxidation of soot,

733   Atmospheric Environment, 36, 1827-1832, 10.1016/s1352-2310(02)00141-3, 2002.

734   Decesari, S., Fuzzi, S., Facchini, M. C., Mircea, M., Emblico, L., Cavalli, F., Maenhaut,

735   W., Chi, X., Schkolnik, G., Falkovich, A., Rudich, Y., Claeys, M., Pashynska, V., Vas,

736   G., Kourtchev, I., Vermeylen, R., Hoffer, A., Andreae, M. O., Tagliavini, E., Moretti, F.,

737   and Artaxo, P.: Characterization of the organic composition of aerosols from Rondonia,

738   Brazil, during the LBA-SMOCC 2002 experiment and its representation through

739   model compounds, Atmospheric Chemistry and Physics, 6, 375-402, 2006.

740   Dick, W. D., Saxena, P., and McMurry, P. H.: Estimation of water uptake by organic

741   compounds in submicron aerosols measured during the Southeastern Aerosol and

742   Visibility Study, Journal of Geophysical Research-Atmospheres, 105, 1471-1479,

743   10.1029/1999jd901001, 2000.

744   Dinar, E., Mentel, T. F., and Rudich, Y.: The density of humic acids and humic like

745   substances (HULIS) from fresh and aged wood burning and pollution aerosol particles,

746   Atmospheric Chemistry and Physics, 6, 5213-5224, 2006a.

747   Dinar, E., Taraniuk, I., Graber, E. R., Katsman, S., Moise, T., Anttila, T., Mentel, T. F.,

748   and Rudich, Y.: Cloud Condensation Nuclei properties of model and atmospheric

749   HULIS, Atmospheric Chemistry and Physics, 6, 2465-2481, 2006b.

750   Dinar, E., Taraniuk, I., Graber, E. R., Anttila, T., Mentel, T. F., and Rudich, Y.:

751   Hygroscopic growth of atmospheric and model humic-like substances, Journal of

752   Geophysical Research, 112, 10.1029/2006jd007442, 2007.

753   Djikaev, Y. S., Bowles, R., Reiss, H., Hameri, K., Laaksonen, A., and Vakeva, M.: Theory

754   of size dependent deliquescence of nanoparticles: Relation to heterogeneous nucleation

755   and comparison with experiments, Journal of Physical Chemistry B, 105, 7708-7722,

756   10.1021/jp010537e, 2001.

757   Duplissy, J., Gysel, M., Sjogren, S., Meyer, N., Good, N., Kammermann, L., Michaud, V.,

758   Weigel, R., dos Santos, S. M., Gruening, C., Villani, P., Laj, P., Sellegri, K., Metzger,

759   A., McFiggans, G. B., Wehrle, G., Richter, R., Dommen, J., Ristovski, Z.,

760   Baltensperger, U., and Weingartner, E.: Intercomparison study of six HTDMAs: results

761   and recommendations, Atmospheric Measurement Techniques, 2, 363-378, 2009.

762   Dusek, U., Frank, G. P., Massling, A., Zeromskiene, K., Iinuma, Y., Schmid, O., Helas, G.,

763   Hennig, T., Wiedensohler, A., and Andreae, M. O.: Water uptake by biomass burning

764   aerosol at sub- and supersaturated conditions: closure studies and implications for the

765   role   of   organics,   Atmospheric   Chemistry   and   Physics,   11,   9519-9532,

766   10.5194/acp-11-9519-2011, 2011.

767   Engling, G., Lee, J. J., Sie, H.-J., Wu, Y.-C., and I, Y.-P.: Anhydrosugar characteristics in

768   biomass smoke aerosol—case study of environmental influence on particle-size of rice

769   straw   burning   aerosol,   Journal   of   Aerosol   Science,   56,   2-14,

770   10.1016/j.jaerosci.2012.10.001, 2013.

771   Fine, P. M., Cass, G. R., and Simoneit, B. R. T.: Organic compounds in biomass smoke

772   from residential wood combustion: Emissions characterization at a continental scale,

773   Journal of Geophysical Research-Atmospheres, 107, 10.1029/2001jd000661, 2002.

774 Fors, E. O., Rissler, J., Massling, A., Svenningsson, B., Andreae, M. O., Dusek, U., Frank,

775   G. P., Hoffer, A., Bilde, M., Kiss, G., Janitsek, S., Henning, S., Facchini, M. C.,

776   Decesari, S., and Swietlicki, E.: Hygroscopic properties of Amazonian biomass

777   burning and European background HULIS and investigation of their effects on surface

778   tension with two models linking H-TDMA to CCNC data, Atmospheric Chemistry and

779   Physics, 10, 5625-5639, 10.5194/acp-10-5625-2010, 2010.

780 Fredenslund, A., Jones, R. L., and Prausnitz, J. M.: GROUP-CONTRIBUTION

781   ESTIMATION   OF   ACTIVITY-COEFFICIENTS   IN   NONIDEAL

782   LIQUID-MIXTURES, Aiche Journal, 21, 1086-1099, 10.1002/aic.690210607, 1975.

783 Freedman, M. A., Baustian, K. J., Wise, M. E., and Tolbert, M. A.: Characterizing the

784   Morphology of Organic Aerosols at Ambient Temperature and Pressure, Analytical

785   Chemistry, 82, 7965-7972, 10.1021/ac101437w, 2010.

786 Frosch, M., Prisle, N. L., Bilde, M., Varga, Z., and Kiss, G.: Joint effect of organic acids

787   and inorganic salts on cloud droplet activation, Atmospheric Chemistry and Physics, 11,

788   3895-3911, 10.5194/acp-11-3895-2011, 2011.

789 Fu, P. Q., Kawamura, K., and Barrie, L. A.: Photochemical and Other Sources of Organic

790   Compounds in the Canadian High Arctic Aerosol Pollution during Winter-Spring,

791   Environmental Science & Technology, 43, 286-292, 10.1021/es803046q, 2009.

792 Fuzzi, S., Decesari, S., Facchini, M. C., Matta, E., Mircea, M., and Tagliavini, E.: A

793   simplified model of the water soluble organic component of atmospheric aerosols,

794   Geophysical Research Letters, 28, 4079-4082, 10.1029/2001gl013418, 2001.

795 Gao, Y., Yu, L. E., and Chen, S. B.: Effects of organics on efflorescence relative humidity

796   of ammonium sulfate or sodium chloride particles, Atmospheric Environment, 42,

797 4433-4445, 10.1016/j.atmosenv.2008.02.002, 2008.

798 Gysel, M., Weingartner, E., and Baltensperger, U.: Hygroscopicity of aerosol particles at

799 low temperatures. 2. Theoretical and experimental hygroscopic properties of laboratory

800 generated aerosols, Environmental Science & Technology, 36, 63-68,

801 10.1021/es010055g, 2002.

802 Gysel, M., Weingartner, E., Nyeki, S., Paulsen, D., Baltensperger, U., Galambos, I., and

803 Kiss, G.: Hygroscopic properties of water-soluble matter and humic-like organics in

804 atmospheric fine aerosol, Atmospheric Chemistry and Physics, 4, 35-50, 2004.

805 Ha, Z. Y., and Chan, C. K.: The water activities of MgCl2, Mg(NO3)(2), MgSO4, and

806 their mixtures, Aerosol Science and Technology, 31, 154-169,

807 10.1080/027868299304219, 1999.

808 Hameri, K., Vakeva, M., Hansson, H. C., and Laaksonen, A.: Hygroscopic growth of

809 ultrafine ammonium sulphate aerosol measured using an ultrafine tandem differential

810 mobility analyzer, Journal of Geophysical Research-Atmospheres, 105, 22231-22242,

811 10.1029/2000jd900220, 2000.

812 Hameri, K., Charlson, R., and Hansson, H. C.: Hygroscopic properties of mixed

813 ammonium sulfate and carboxylic acids particles, Aiche Journal, 48, 1309-1316,

814 10.1002/aic.690480617, 2002.

815 Hanford, K. L., Mitchem, L., Reid, J. P., Clegg, S. L., Topping, D. O., and McFiggans, G.

816 B.: Comparative thermodynamic studies of aqueous glutaric acid, ammonium sulfate

817 and sodium chloride aerosol at high humidity, Journal of Physical Chemistry A, 112,

818 9413-9422, 10.1021/jp802520d, 2008.

819 Hansen, H. K., Rasmussen, P., Fredenslund, A., Schiller, M., and Gmehling, J.:

820   vapor-liquid-equlibria by unifac group contribution. 5. revision and extension,

821   Industrial & Engineering Chemistry Research, 30, 2352-2355, 10.1021/ie00058a017,

822   1991.

823   Hatch, C. D., Gierlus, K. M., Zahardis, J., Schuttlefield, J., and Grassian, V. H.: Water

824   uptake of humic and fulvic acid: measurements and modelling using single parameter

825   Köhler theory, Environmental Chemistry, 6, 380, 10.1071/en09083, 2009.

826   Heintzenberg, J. and Charlson, R. J. (eds.): Clouds in the perturbed climate system: their

827   relationship to energy balance, atmospheric dynamics, and precipitation, Struengmann

828   Forum Report, vol. 2., The MIT Press, Cambridge, MA, USA, 2009.

829   Henning, S., Rosenorn, T., D'Anna, B., Gola, A. A., Svenningsson, B., and Bilde, M.:

830   Cloud droplet activation and surface tension of mixtures of slightly soluble organics

831   and inorganic salt, Atmospheric Chemistry and Physics, 5, 575-582, 2005.

832   Henning, S., Wex, H., Hennig, T., Kiselev, A., Snider, J. R., Rose, D., Dusek, U., Frank,

833   G. P., Pöschl, U., Kristensson, A., Bilde, M., Tillmann, R., Kiendler-Scharr, A., Mentel,

834   T. F., Walter, S., Schneider, J., Wennrich, C., and Stratmann, F.: Soluble mass,

835   hygroscopic growth, and droplet activation of coated soot particles during LACIS

836   Experiment in November (LExNo), Journal of Geophysical Research, 115,

837   10.1029/2009jd012626, 2010.

838   Hersey, S. P., Craven, J. S., Metcalf, A. R., Lin, J., Lathem, T., Suski, K. J., Cahill, J. F.,

839   Duong, H. T., Sorooshian, A., Jonsson, H. H., Shiraiwa, M., Zuend, A., Nenes, A.,

840   Prather, K. A., Flagan, R. C., and Seinfeld, J. H.: Composition and hygroscopicity of

841   the Los Angeles Aerosol: CalNex, Journal of Geophysical Research: Atmospheres, 118,

842   3016-3036, 10.1002/jgrd.50307, 2013.

843   Hoffer, A., Gelencser, A., Guyon, P., Kiss, G., Schmid, O., Frank, G. P., Artaxo, P., and

844   Andreae, M. O.: Optical properties of humic-like substances (HULIS) in

845   biomass-burning aerosols, Atmospheric Chemistry and Physics, 6, 3563-3570, 2006.

846   Holmes, B. J., and Petrucci, G. A.: Oligomerization of levoglucosan by Fenton chemistry

847   in proxies of biomass burning aerosols, Journal of Atmospheric Chemistry, 58,

848   151-166, 10.1007/s10874-007-9084-8, 2007.

849   Iinuma, Y., Brüggemann, E., Gnauk, T., Müller, K., Andreae, M. O., Helas, G., Parmar, R.,

850   and Herrmann, H.: Source characterization of biomass burning particles: The

851   combustion of selected European conifers, African hardwood, savanna grass, and

852   German and Indonesian peat, Journal of Geophysical Research, 112,

853   10.1029/2006jd007120, 2007.

854   Jedelsk´y, J., Hnedkovskí, L., Hyncica, P., and Cibulka, I.: Partial molar volumes of

855   organic solutes in water. IV. Benzoic and hydroxybenzoic acids at temperatures from T

856   D 298K to T D 498 K and pressures up to 30MPa, J. Chem. Thermodyn., 32,

857   1299-1310, 2000.

858   Jokinen, V., and Makela, J. M.: Closed-loop arrangement with critical orifice for DMA

859   sheath excess flow system, Journal of Aerosol Science, 28, 643-648,

860   10.1016/s0021-8502(96)00457-0, 1997.

861   Jung, J., and Kim, Y. J.: Tracking sources of severe haze episodes and their

862   physicochemical and hygroscopic properties under Asian continental outflow:

863   Long-range transport pollution, postharvest biomass burning, and Asian dust, Journal

864   of Geophysical Research, 116, 10.1029/2010jd014555, 2011.

865   Jung, J., Kim, Y. J., Aggarwal, S. G., and Kawamura, K.: Hygroscopic property of

866   water-soluble organic-enriched aerosols in Ulaanbaatar, Mongolia during the cold

867   winter   of   2007,   Atmospheric   Environment,   45,   2722-2729,

868   10.1016/j.atmosenv.2011.02.055, 2011a.

869   Jung, J. S., Kim, Y. J., Aggarwal, S. G., and Kawamura, K.: Hygroscopic property of

870   water-soluble organic-enriched aerosols in Ulaanbaatar, Mongolia during the cold

871   winter   of   2007,   Atmospheric   Environment,   45,   2722-2729,

872   10.1016/j.atmosenv.2011.02.055, 2011b.

873   Kerminen, V. M.: The effects of particle chemical character and atmospheric processes on

874   particle   hygroscopic   properties,   Journal   of   Aerosol   Science,   28,   121-132,

875   10.1016/s0021-8502(96)00069-9, 1997.

876   Kiss, G., Tombácz, E., and Hansson, H.-C.: Surface Tension Effects of Humic-Like

877   Substances in the Aqueous Extract of Tropospheric Fine Aerosol, Journal of

878   Atmospheric Chemistry, 50, 279-294, 10.1007/s10874-005-5079-5, 2005.

879   Koehler, K. A., Kreidenweis, S. M., DeMott, P. J., Prenni, A. J., Carrico, C. M., Ervens,

880   B., and Feingold, G.: Water activity and activation diameters from hygroscopicity data

881   - Part II: Application to organic species, Atmospheric Chemistry and Physics, 6,

882   795-809, 2006.

883   Kreidenweis, S. M., Koehler, K., DeMott, P. J., Prenni, A. J., Carrico, C., and Ervens, B.:

884   Water activity and activation diameters from hygroscopicity data - Part I: Theory and

885   application to inorganic salts, Atmospheric Chemistry and Physics, 5, 1357-1370,

886   2005.

887   Lienhard, D. M., Bones, D. L., Zuend, A., Krieger, U. K., Reid, J. P., and Peter, T.:

888   Measurements of thermodynamic and optical properties of selected aqueous organic

889 and organic-inorganic mixtures of atmospheric relevance, The journal of physical

890 chemistry. A, 116, 9954-9968, 10.1021/jp3055872, 2012.

891 Lightstone, J. M., Onasch, T. B., Imre, D., and Oatis, S.: Deliquescence, efflorescence,

892 and water activity in ammonium nitrate and mixed ammonium nitrate/succinic acid

893 microparticles, Journal of Physical Chemistry A, 104, 9337-9346, 10.1021/jp002137h,

894 2000.

895 Lohmann, U., and Feichter, J.: Global indirect aerosol effects: a review, Atmospheric

896 Chemistry and Physics, 5, 715-737, 2005.

897 Malm, W. C., and Kreidenweis, S. M.: The effects of models of aerosol hygroscopicity on

898 the apportionment of extinction, Atmospheric Environment, 31, 1965-1976,

899 10.1016/s1352-2310(96)00355-x, 1997.

900 Marcolli, C. B. L. and Peter, T.: Mixing of the organic aerosol fractions: liquids as the

901 thermodynamically stable phases, J. Phys. Chem. A, 108, 2216-2224, 2004.

902 Martin, S. T., Andreae, M. O., Artaxo, P., Baumgardner, D., Chen, Q., Goldstein, A. H.,

903 Guenther, A., Heald, C. L., Mayol-Bracero, O. L., McMurry, P. H., Pauliquevis, T.,

904 Pöschl, U., Prather, K. A., Roberts, G. C., Saleska, S. R., Silva Dias, M. A., Spracklen,

905 D. V., Swietlicki, E., and Trebs, I.: Sources and properties of Amazonian aerosol

906 particles, Reviews of Geophysics, 48, 10.1029/2008rg000280, 2010.

907 Maskey, S., Chong, K. Y., Kim, G., Kim, J.-S., Ali, A., and Park, K.: Effect of mixing

908 structure on the hygroscopic behavior of ultrafine ammonium sulfate particles mixed

909 with succinic acid and levoglucosan, Particuology, 13, 27-34,

910 10.1016/j.partic.2013.08.004, 2014.

911 Mikhailov, E., Vlasenko, S., Niessner, R., and Poschl, U.: Interaction of aerosol particles

912   composed of protein and salts with water vapor: hygroscopic growth and

913   microstructural rearrangement, Atmospheric Chemistry and Physics, 4, 323-350, 2004.

914 Mikhailov, E., Vlasenko, S., Martin, S. T., Koop, T., and Poschl, U.: Amorphous and

915   crystalline aerosol particles interacting with water vapor: conceptual framework and

916   experimental evidence for restructuring, phase transitions and kinetic limitations,

917   Atmospheric Chemistry and Physics, 9, 9491-9522, 2009.

918 Mikhailov, E. F., Vlasenko, S. S., and Ryshkevich, T. I.: Influence of chemical

919   composition and microstructure on the hygroscopic growth of pyrogenic aerosol,

920   Izvestiya, Atmospheric and Oceanic Physics, 44, 416-431,

921   10.1134/s0001433808040038, 2008.

922 Mirabel, P., Reiss, H., and Bowles, R. K.: A theory for the deliquescence of small

923   particles, Journal of Chemical Physics, 113, 8200-8205, 10.1063/1.1315993, 2000.

924 Mochida, M. and Kawamura, K.: Hygroscopic properties of levoglucosan and related

925   organic compounds characteristic to biomass burning aerosol particles, J. Geophys.

926   Res.-Atmos., 109, D21202, doi:10.1029/2004jd004962, 2004.

927 Narukawa, M., Kawamura, K., Takeuchi, N., and Nakajima, T.: Distribution of

928   dicarboxylic acids and carbon isotopic compositions in aerosols from 1997 Indonesian

929   forest fires, Geophysical Research Letters, 26, 3101-3104, 10.1029/1999gl010810,

930   1999.

931 Novakov, T., and Corrigan, C. E.: Cloud condensation nucleus activity of the organic

932   component of biomass smoke particles, Geophysical Research Letters, 23, 2141-2144,

933   10.1029/96gl01971, 1996.

934 Onasch, T. B., Siefert, R. L., Brooks, S. D., Prenni, A. J., Murray, B., Wilson, M. A., and

935   Tolbert, M. A.: Infrared spectroscopic study of the deliquescence and efflorescence of

936   ammonium sulfate aerosol as a function of temperature, Journal of Geophysical

937   Research-Atmospheres, 104, 21317-21326, 10.1029/1999jd900384, 1999.

938   Pöschl, U.: Atmospheric Aerosols: Composition, Transformation, Climate and Health

939   Effects, Angewandte Chemie International Edition, 44, 7520-7540,

940   10.1002/anie.200501122, 2005.

941   Pandis, S. N., Wexler, A. S., and Seinfeld, J. H.: DYNAMICS OF TROPOSPHERIC

942   AEROSOLS, Journal of Physical Chemistry, 99, 9646-9659, 10.1021/j100024a003,

943   1995.

944   Peng, C., Chan, M. N., and Chan, C. K.: The hygroscopic properties of dicarboxylic and

945   multifunctional acids: measurements and UNIFAC predictions, Environ. Sci. Technol.,

946   35, 4495–4501, 2001.

947   Petters, M. D., Carrico, C. M., Kreidenweis, S. M., Prenni, A. J., DeMott, P. J., Collett, J.

948   L., and Moosmüller, H.: Cloud condensation nucleation activity of biomass burning

949   aerosol, Journal of Geophysical Research, 114, 10.1029/2009jd012353, 2009.

950   Pilinis, C., Pandis, S. N., and Seinfeld, J. H.: sensitivity of direct climate forcing by

951   atmospheric aerosols to aerosol-size and composition, Journal of Geophysical

952   Research-Atmospheres, 100, 18739-18754, 10.1029/95jd02119, 1995.

953   Pope, F. D., Dennis-Smither, B. J., Griffiths, P. T., Clegg, S. L., and Cox, R. A.: Studies of

954   Single Aerosol Particles Containing Malonic Acid, Glutaric Acid, and Their Mixtures

955   with Sodium Chloride. I. Hygroscopic Growth, Journal of Physical Chemistry A, 114,

956   5335-5341, 10.1021/jp100059k, 2010a.

957   Pope, F. D., Harper, L., Dennis-Smither, B. J., Griffiths, P. T., Clegg, S. L., and Cox, R.

958 A.: Laboratory and modelling study of the hygroscopic properties of two model humic

959 acid aerosol particles, Journal of Aerosol Science, 41, 457-467,

960 10.1016/j.jaerosci.2010.02.012, 2010b.

961 Psichoudaki, M., and Pandis, S. N.: Atmospheric aerosol water-soluble organic carbon

962 measurement: a theoretical analysis, Environ Sci Technol, 47, 9791-9798,

963 10.1021/es402270y, 2013.

964 Qiu, C., and Zhang, R. Y.: Multiphase chemistry of atmospheric amines, Physical

965 Chemistry Chemical Physics, 15, 5738-5752, 10.1039/c3cp43446j, 2013.

966 Raymond, T. M., and Pandis, S. N.: Cloud activation of single-component organic aerosol

967 particles, Journal of Geophysical Research-Atmospheres, 107, 10.1029/2002jd002159,

968 2002.

969 Rissler, J., Vestin, A., Swietlicki, E., Fisch, G., Zhou, J., Artaxo, P., and Andreae, M. O.:

970 Size distribution and hygroscopic properties of aerosol particles from dry-season

971 biomass burning in Amazonia, Atmospheric Chemistry and Physics, 6, 471-491, 2006.

972 Rissler, J., Svenningsson, B., Fors, E. O., Bilde, M., and Swietlicki, E.: An evaluation and

973 comparison of cloud condensation nucleus activity models: Predicting particle critical

974 saturation from growth at subsaturation, Journal of Geophysical Research, 115,

975 10.1029/2010jd014391, 2010.

976 Roberts, G. C., Andreae, M. O., Maenhaut, W., and Fernandez-Jimenez, M. T.:

977 Composition and sources of aerosol in a central African rain forest during the dry

978 season, Journal of Geophysical Research-Atmospheres, 106, 14423-14434,

979 10.1029/2000jd900774, 2001.

980   Roberts, G. C., Artaxo, P., Zhou, J. C., Swietlicki, E., and Andreae, M. O.: Sensitivity of

981   CCN spectra on chemical and physical properties of aerosol: a case study from the

982   Amazon Basin, J. Geophys. Res.-Atmos., 107, 8070, doi:10.1029/2001jd000583, 2002.

983   Roberts, G. C., Nenes, A., Seinfeld, J. H., and Andreae, M. O.: Impact of biomass

984   burning on cloud properties in the Amazon Basin, J. Geophys. Res.-Atmos., 108, 4062,

985   doi:10.1029/2001jd000985, 2003.

986   Ruellan, S., Cachier, H., Gaudichet, A., Masclet, P., and Lacaux, J. P.: Airborne aerosols

987   over central Africa during the experiment for regional sources and sinks of oxidants

988   (EXPRESSO), Journal of Geophysical Research-Atmospheres, 104, 30673-30690,

989   10.1029/1999jd900804, 1999.

990   Russell, L. M., and Ming, Y.: Deliquescence of small particles, Journal of Chemical

991   Physics, 116, 311-321, 10.1063/1.1420727, 2002.

992   Samburova, V., Hallar, A. G., Mazzoleni, L. R., Saranjampour, P., Lowenthal, D., Kohl, S.

993   D., and Zielinska, B.: Composition of water-soluble organic carbon in non-urban

994   atmospheric aerosol collected at the Storm Peak Laboratory, Environmental Chemistry,

995   10, 370, 10.1071/en13079, 2013.

996   Schultz, M. G., Heil, A., Hoelzemann, J. J., Spessa, A., Thonicke, K., Goldammer, J. G.,

997   Held, A. C., Pereira, J. M. C., and van het Bolscher, M.: Global wildland fire emissions

998   from 1960 to 2000, Glob. Biogeochem. Cy., 22, GB2002, doi:10.1029/2007GB003031,

999   2008.

1000   Shi, Y. J., Ge, M. F., and Wang, W. G.: Hygroscopicity of internally mixed aerosol

1001   particles containing benzoic acid and inorganic salts, Atmospheric Environment, 60,

1002   9-17, 10.1016/j.atmosenv.2012.06.034, 2012.

1003 Shiraiwa, M., Zuend, A., Bertram, A. K., and Seinfeld, J. H.: Gas-particle partitioning of

1004   atmospheric aerosols: interplay of physical state, non-ideal mixing and morphology,

1005   Physical Chemistry Chemical Physics, 15, 11441-11453, 10.1039/c3cp51595h, 2013.

1006 Simoneit, B. R. T., Schauer, J. J., Nolte, C. G., Oros, D. R., Elias, V. O., Fraser, M. P.,

1007   Rogge, W. F., and Cass, G. R.: Levoglucosan, a tracer for cellulose in biomass burning

1008   and   atmospheric   particles,   Atmospheric   Environment,   33,   173-182,

1009   10.1016/s1352-2310(98)00145-9, 1999.

1010 Sjogren, S., Gysel, M., Weingartner, E., Baltensperger, U., Cubison, M. J., Coe, H.,

1011   Zardini, A. A., Marcolli, C., Krieger, U. K., and Peter, T.: Hygroscopic growth and

1012   water uptake kinetics of two-phase aerosol particles consisting of ammonium sulfate,

1013   adipic   and   humic   acid   mixtures,   Journal   of   Aerosol   Science,   38,   157-171,

1014   10.1016/j.jaerosci.2006.11.005, 2007.

1015 Sloane, C. S., and Wolff, G. T.: Prediction of ambient light-scattering using a physical

1016   model responsive to relative-humidity-validation with measurements from detroit,

1017   Atmospheric Environment, 19, 669-680, 10.1016/0004-6981(85)90046-0, 1985.

1018 Song, M., Marcolli, C., Krieger, U. K., Zuend, A., and Peter, T.: Liquid-liquid phase

1019   separation   and   morphology   of   internally   mixed   dicarboxylic   acids/ammonium

1020   sulfate/water   particles,   Atmospheric   Chemistry   and   Physics,   12,   2691-2712,

1021   10.5194/acp-12-2691-2012, 2012.

1022 Stokes, R. H. and Robinson, R. A.: Interactions in aqueous nonelectrolyte solutions. I.

1023   Solute-solvent equilibria, J. Phys. Chem., 70, 2126–2130, 1966.

1024 Stolzenburg, M. R., and McMurry, P. H.: Equations governing single and tandem DMA

1025   configurations and a new lognormal approximation to the transfer function, Aerosol

1026   Science and Technology, 42, 421-432, 10.1080/02786820802157823, 2008.

1027   Svenningsson, B., Rissler, J., Swietlicki, E., Mircea, M., Bilde, M., Facchini, M. C.,

1028   Decesari, S., Fuzzi, S., Zhou, J., Monster, J., and Rosenorn, T.: Hygroscopic growth

1029   and critical supersaturations for mixed aerosol particles of inorganic and organic

1030   compounds of atmospheric relevance, Atmospheric Chemistry and Physics, 6,

1031   1937-1952, 2006.

1032   Tuckermann, R. and Cammenga, H. K.: The surface tension of aqueous solutions of some

1033   atmospheric water-soluble organic compounds, Atmos. Environ., 38 (36), 6135–6138,

1034   2004.

1035   van der Werf, G. R., Randerson, J. T., Giglio, L., Collatz, G. J., Kasibhatla, P. S., and

1036   Arellano, A. F.: Interannual variability in global biomass burning emissions from 1997

1037   to 2004, Atmospheric Chemistry and Physics, 6, 3423-3441, 2006.

1038   Vestin, A., Rissler, J., Swietlicki, E., Frank, G. P., and Andreae, M. O.: Cloud-nucleating

1039   properties of the Amazonian biomass burning aerosol: Cloud condensation nuclei

1040   measurements and modeling, Journal of Geophysical Research, 112,

1041   10.1029/2006jd008104, 2007.

1042   Wise, M. E, Surratt, J. D, Curtis, D. B, Shilling, J. E, and Tolbert, M. A.: Hygroscopic

1043   growth of ammonium sulfate/dicarboxylic acids, J. Geophys. Res., 108(D20), 4638,

1044   doi:10.1029/2003JD003775, 2003.

1045   Wu, Z. J., Nowak, A., Poulain, L., Herrmann, H., and Wiedensohler, A.: Hygroscopic

1046   behavior of a tmospherically relevant water-soluble carboxylic salts and their influence

1047   on the water uptake of ammonium sulfate, Atmospheric Chemistry and Physics, 11,

1048   12617-12626, 10.5194/acp-11-12617-2011, 2011.

1049   Yates III, L. M. and Wandruszka, R. V.: Decontamination of polluted water by treatment

1050   with a crude humic acid blend, Environ. Sci. Technol., 33, 2076-2080, 1999.

1051   Yeung, M. C., and Chan, C. K.: Water Content and Phase Transitions in Particles of

1052   Inorganic and Organic Species and their Mixtures Using Micro-Raman Spectroscopy,

1053   Aerosol Science and Technology, 44, 269-280, 10.1080/02786820903583786, 2010.

1054   Zamora, I. R., Tabazadeh, A., Golden, D. M., and Jacobson, M. Z.: Hygroscopic growth

1055   of common organic aerosol solutes, including humic substances, as derived from water

1056   activity measurements, Journal of Geophysical Research: Atmospheres, 116, n/a-n/a,

1057   10.1029/2011jd016067, 2011.

1058   Zamora, I. R., and Jacobson, M. Z.: Measuring and modeling the hygroscopic growth of

1059   two humic substances in mixed aerosol particles of atmospheric relevance,

1060   Atmospheric Chemistry and Physics, 13, 8973-8989, 10.5194/acp-13-8973-2013,

1061   2013.

1062   Zardini, A. A., Sjogren, S., Marcolli, C., Krieger, U. K., Gysel, M., Weingartner, E.,

1063   Baltensperger, U., and Peter, T.: A combined particle trap/HTDMA hygroscopicity

1064   study of mixed inorganic/organic aerosol particles, Atmospheric Chemistry and

1065   Physics, 8, 5589-5601, 2008.

1066   Zhang, Y. H., and Chan, C. K.: Study of contact ion pairs of supersaturated magnesium

1067   sulfate solutions using raman scattering of levitated single droplets, Journal of Physical

1068   Chemistry A, 104, 9191-9196, 10.1021/jp0013659, 2000.

1069   Zhou, J. C., Swietlicki, E., Hansson, H. C., and Artaxo, P.: Submicrometer aerosol

1070   particle size distribution and hygroscopic growth measured in the Amazon rain forest

1071   during the wet season, Journal of Geophysical Research-Atmospheres, 107,

1072   10.1029/2000jd000203, 2002.

1073   Zuend, A., Marcolli, C., Luo, B. P., and Peter, T.: A thermodynamic model of mixed

1074   organic-inorganic aerosols to predict activity coefficients, Atmospheric Chemistry and

1075   Physics, 8, 4559-4593, 2008.

1076   Zuend, A., Marcolli, C., Peter, T., and Seinfeld, J. H.: Computation of liquid-liquid

1077   equilibria and phase stabilities: implications for RH-dependent gas/particle partitioning

1078   of organic-inorganic aerosols, Atmospheric Chemistry and Physics, 10, 7795-7820,

1079   10.5194/acp-10-7795-2010, 2010.

1080   Zuend, A., Marcolli, C., Booth, A. M., Lienhard, D. M., Soonsin, V., Krieger, U. K.,

1081   Topping, D. O., McFiggans, G., Peter, T., and Seinfeld, J. H.: New and extended

1082   parameterization of the thermodynamic model AIOMFAC: calculation of activity

1083   coefficients for organic-inorganic mixtures containing carboxyl, hydroxyl, carbonyl,

1084   ether, ester, alkenyl, alkyl, and aromatic functional groups, Atmospheric Chemistry and

1085   Physics, 11, 9155-9206, 10.5194/acp-11-9155-2011, 2011.

1086   Zuend, A., and Seinfeld, J. H.: Modeling the gas-particle partitioning of secondary

1087   organic aerosol: the importance of liquid-liquid phase separation, Atmospheric

1088   Chemistry and Physics, 12, 3857-3882, 10.5194/acp-12-3857-2012, 2012.

1089   Zuend, A., and Seinfeld, J. H.: A practical method for the calculation of liquid–liquid

1090   equilibria in multicomponent organic–water–electrolyte systems using

1091   physicochemical constraints, Fluid Phase Equilibria, 337, 201-213,

1092   10.1016/j.fluid.2012.09.034, 2013.

1093

1094

1095 **Table 1.** Substances and their physical properties used in this work.

1096

Chemical compound	Chemical formula	Molar Mass [g mol^{-1}]	Density in solid and liquid state [g cm^{-3}]	Solubility g/100cm^3 H$_2$O	Solution surface Tension [J m^{-2}]	Manufacture
Ammonium sulfate	(NH$_4$)$_2$SO$_4$	132.140	1.770[a], 1.550[b]	74.400 (at 20℃)	0.072	Alfa Aesar, 99.95%
Levoglucosan	C$_6$H$_{10}$O$_5$	162.100	1.618[c] 1.512[d]		0.073[e] (0.01-10 mg/mL)	Aldrich, 99%
4-Hydroxyben zoic acid	C$_7$H$_6$O$_3$	138.100	1.460 1.372[f]	0.675(at 25 ℃)	0.070[g]	Alfa Aesar, 99.99%
Humic acids		NA	0.800[h]	NA	0.073[i]	Aldrich, 99%

1097

1098   [a] Clegg and Wexler (2011a);

1099   [b] Lienhard et al. (2012);

1100   [c] Tuckermann and Cammenga (2004);

1101   [d] Jedelsk´y et al. (2000);

1102   [e] Kiss et al. (2005);

1103   [f] Yates III and Wandruszka (1999);

1104   [i] Mikhailov et al. (2008).

1105

1106

1107

1108

1109

1110 **Table 2.** Initial dry diameter ($D_{h,dry}$) (RH < 5 %) and minimum mobility diameter ($D_{h,min}$)
1111 in hydration (h) mode of the HTDMA experiments.

1112

Aerosol type	$D_{h,dry\ (nm)}$	$D_{h,min\ (nm)}$
Ammonium sulfate	100.6	99.5
Levoglucosan	99.8	99.6
Humic acid	100.4	100.3
4-Hydroxybenzoic acid	100.2	95.0

1113

1114

1115

1116

1117

1118

1119

1120

1121

1122

1123

1124

1125

1126

1127

1128

1129

1130

1131

1132

1133

1134   **Table 3.** Coefficients (a, b, c) of the fitted growth curve parameterization to measured
1135   growth factor data using Eq. (1). Measured growth factors of D_0 nm particles used in Eq.
1136   (1) were first corrected for the Kelvin effect.
1137

Chemical compounds	a	b	c
Levoglucosan	0.45602	-0.69869	0.44755
4-Hydroxybenzoic acid $D_0 = D_{h,dry}$	-0.14061	0.22767	-0.09526
Humic acid	0.33579	-0.60172	0.40850

1138

1139

1140

1141

1142

1143

1144

1145

1146

1147

1148

1149

1150

1151

1152

1153 **Table 4.** The chemical composition of biomass-burning model mixtures studied, given as

1154 mass percentages (wt %).

Mixture name	Ammonium sulfate	Levoglucosan	4-Hydroxybenzoic	Humic acid
Mix-bio-dry	68.0%	26.0%	3.0%	3.0%
Mix-bio-wet	87.2%	9.2%	1.5%	2.1%

1155

1156

1157

1158

1159

1160

1161

1162

1163

1164

1165

1166

1167

1168

1169

1170
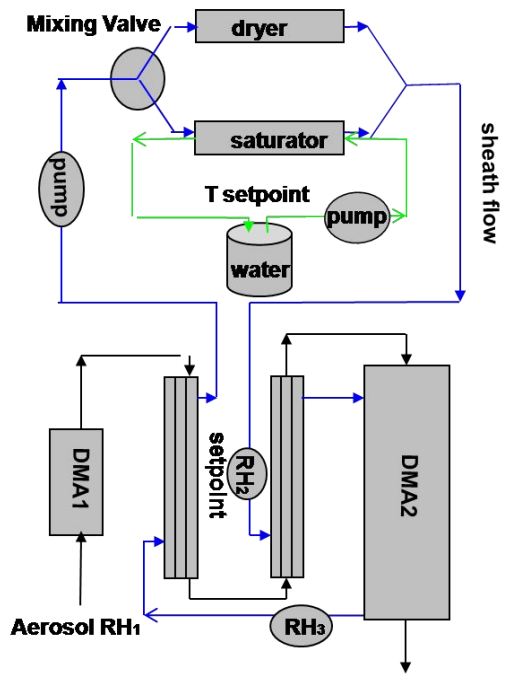
1171

1172 **Fig. 1.** Schematic of the hygroscopicity tandem different mobility analyzer (HTDMA) system.

1173

1174

1175

1176

1177

1178

1179

1180
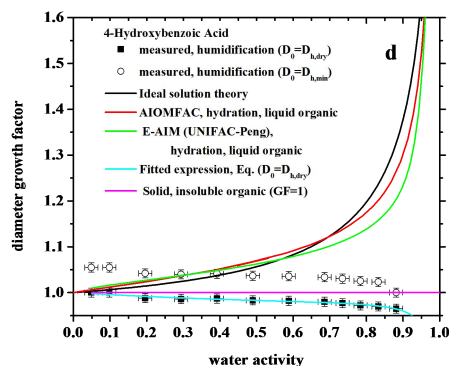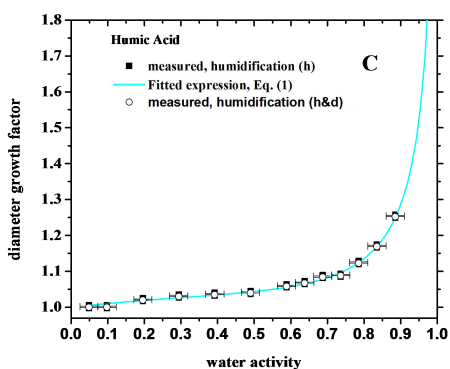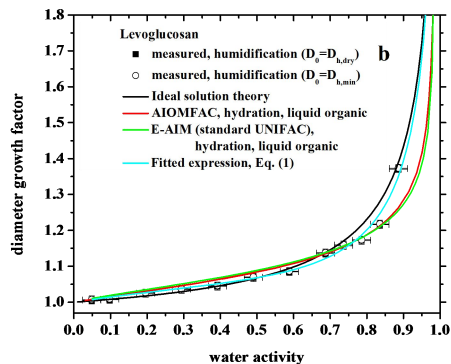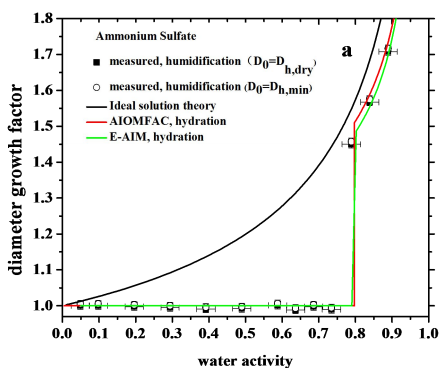
1181

1182

1183   **Fig. 2.** Hygroscopic diameter growth factor (GF) for D_0 (initial dry diameter RH < 5 %) aerosol particles.

1184   The measurements, model calculations, and fitted expression Eq. (1) represent conditions of particle growth

1185   during a hydration experiment from 5 % to 90 % RH at 298.15 K. Measured growth factors are corrected

1186   for the Kelvin effect and and therefore shown vs. water activity. Symbols: measured GF are shown with

1187   respect to $D_0 = D_{h, dry}$ (black squares) or $D_0 = D_{h\&d,min}$ (open circles). Systems: **(a)** ammonium sulfate **(b)**

1188   levoglucosan, **(c)** humic acid, and **(4)** 4-hydroxybenzoic acid.

1189

1190

1191

1192

1193
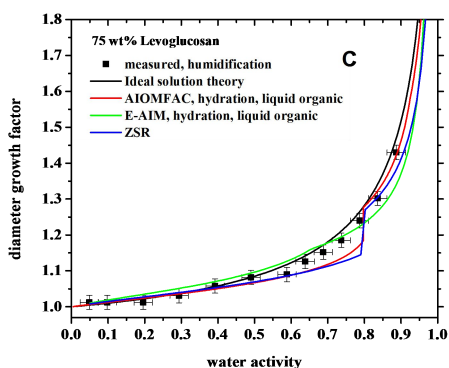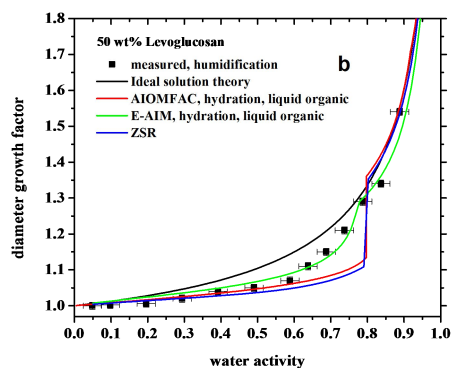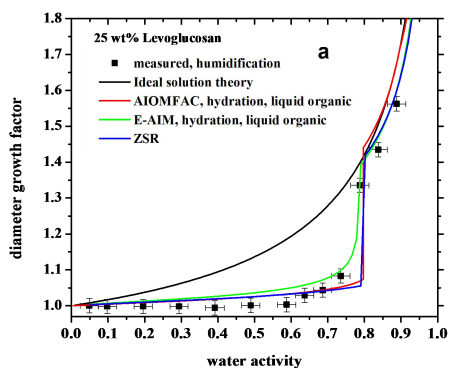
Fig. 3. Hygroscopic growth factors of aerosol particles containing mixtures of levoglucosan with ammonium sulfate at three different dry state mass fractions. The measurements and model calculations represent the particle growth during a hydration experiment from 5 % to 90 % RH at 298.15 K. Measured growth factors are corrected for the Kelvin effect and and therefore shown vs. water activity. Mass ratio of AS: Levoglucosan: **(a)** 3:1, **(b)** 1:1, **(c)** 1:3.
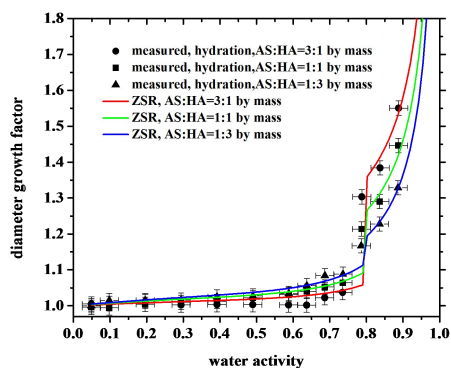
1207

Hygroscopic growth factors of aerosol particles containing mixtures of humic acid (HA) and ammonium sulfate at three different dry state mass ratios. The measurements and ZSR model calculations represent the particle growth during hydration experiments from 5 % to 90 % RH at 298.15 K. Measured growth factors are corrected for the Kelvin effect and and therefore shown vs. water activity.
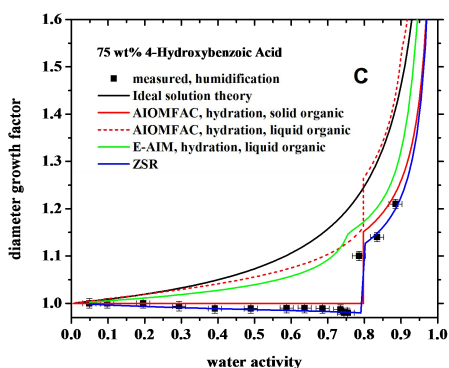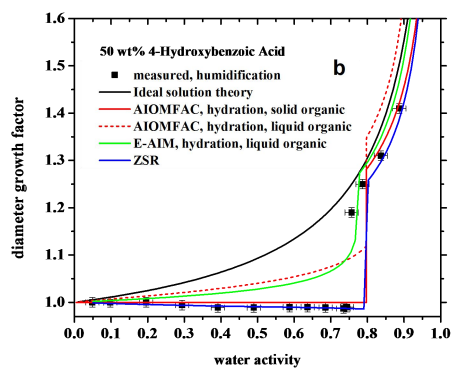
1208
1209
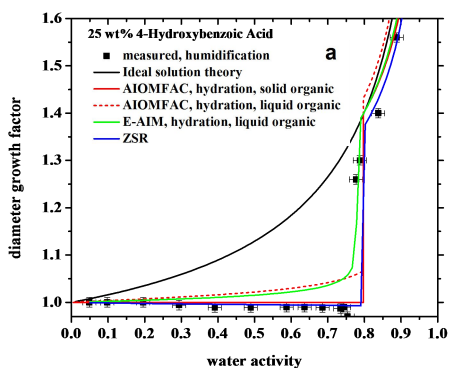1210
1211

1212

1213

1214

1215

1216

1217

1218

1219

1220

1221

1222

1223

1224

1225

1226   **Fig. 5.** Hygroscopic growth factors of aerosol particles containing mixtures of 4-hydroxybenzoic acid with

1227   ammonium sulfate at three different dry mass ratios. The measurements and model calculations represent

1228   particle growth during hydration experiment from 5 % to 90 % RH at 298.15 K. Measured growth factors

1229   are corrected for the Kelvin effect and and therefore shown vs. water activity. Mass ratio of

1230   AS:4-Hydroxybenzoic Acid: **(a)** 3:1, **(b)** 1:1, **(c)** 1:3.
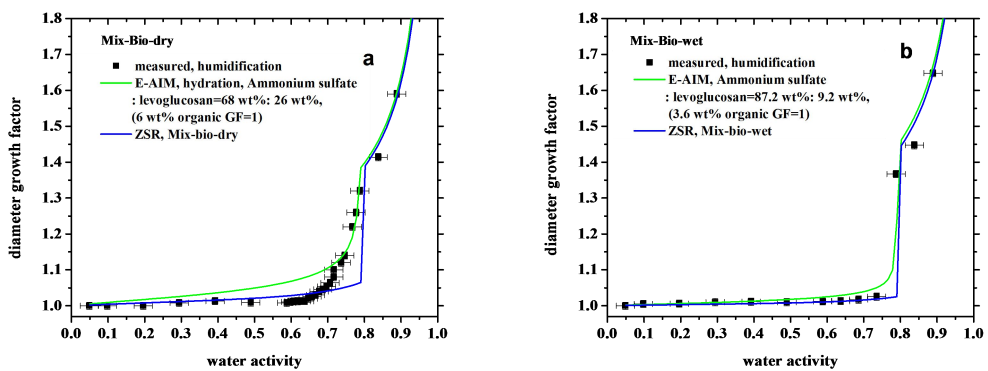
1231

1232

1233

1234

1235

1236

1237

1238 **Fig. 6.** Hygroscopic growth factors of 100nm (dry diameter) particles consisting of mixtures of organic

1239 surrogate compounds with ammonium sulfate representing particles of **(a)** dry and **(b)** wet seasonal periods

1240 in the Amazon . The measurements and model calculations describe the particle growth during hydration

1241 experiments from 5 % to 90 % RH at 298.15 K systems. Measured growth factors are corrected for the

1242 Kelvin effect and and therefore shown vs. water activity.
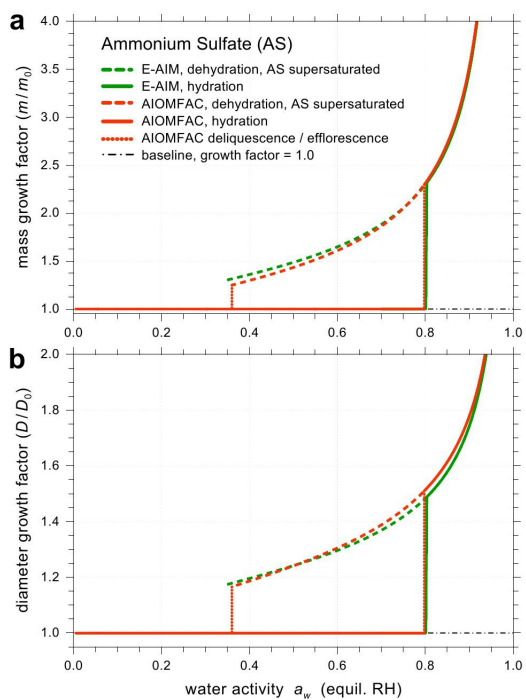
1243

1244

1245

1246

1247

1248

1249

1250

1251

1252

1253

1254

1255 **Fig. 7.** Comparison of E-AIM and AIOMFAC-based mass growth factors (a) and growth diameter growth
1256 factors (b) for the binary ammonium sulfate + water system at 298.15 K.